UNIVERSITAT POLITÈCNICA DE VALÈNCIA

ESCUELA TÉCNICA SUPERIOR INGENIEROS INDUSTRIALES VALENCIA

TRABAJO FIN DE MASTER EN INGENIERÍA INDUSTRIAL

DESIGN OF A CONTROL SYSTEM FOR AN ACTIVE FORWARDER CAB SUSPENSION

AUTOR: PEDRO ESCRIBANO CEBRIÁN

TUTOR: CÉSAR RAMOS FERNÁNDEZ

Curso Académico: 2016-17

Abstract

The forest industry plays an important role in Sweden, and forest machine manufactures are under constant pressure to achieve both high productivity and comfortable operating environment in its products. A forwarder is a forestry vehicle that carries logs which are cut by a harvester. It suffers a lot of low frequency and high amplitude vibrations during the operation because of the rough terrain in forests. Therefore, it is necessary and vital to introduce an active cab suspension system in order to reduce the whole vibrations in the forwarder cab.

The main purposes of this thesis are to develop, implement and test a feasible control strategy for the active cab suspension system as well as verify the controller's performance in terms of vibration reduction and power consumption. This project is focused on the available mechanical rig installed at KTH lab hall, instead of a real forwarder.

A deep study has been carried out on a new valve prototype. Exhausted tests were made to test the performance of this valve under different conditions. From the test results, the valve was tuned in order to get the best performance out of it. Once the valve has been well calibrated, a model of the whole system was estimated by using Black-box estimation. The model has a 96% of matching between the stimulation data and the validation data. Different controllers were designed with this model, and the best one was designed by the gain scheduling method.

The system has a delay of 36 ms, therefore, it was studied how the performance of this controller would increase if the effect of the delay was reduced. The study shows that reducing the delay to around 0-2 ms, the suspension system is able to reduce the vibration from 60% to 90%. Smith Predictor was implemented into the gain scheduling controller in order to reduce the effect of the delay. The results demonstrated a better and more robust performance of the controller with Smith Predictor.

Several test cases were implemented to seek a wide range of possible vibrations that a forwarder could handle in the forest. These tests have been done both in a test rig and in a simulation environment. The final test was conducted by using a real track test model obtained from Skogforsk. This track is used for testing different systems in a test forwarder since it simulates the terrain in a forest. Based on the simulation result, the total disturbance reduction percentages of Smith Predictor controller are 75% for heave, 68% for pitch and 73% for roll, which shows the system reduces the cab vibration. Moreover, the maximum amount of power needed during the forwarder operation is 11.63 kW which is feasible for implementing this system on the actual forwarder.

Key words: forwarder, active suspension, gain scheduling, Smith Predictor

Resumen

La industria forestal desempeña un papel fundamental en Suecia, las manufacturas de máquinas forestales están bajo presión constante para lograr tanto una alta productividad como confort en sus productos. Una Forwarder es un vehículo forestal que transporta troncos cortados en el proceso de talado de árboles. Debido al terreno irregular del bosque, esta sufre muchas vibraciones de baja frecuencia y alta amplitud durante la operación debido. Por lo tanto, es necesario introducir un sistema de suspensión para la cabina con el fin de reducir lo máximo posible todo tipo de vibraciones en dicha cabina.

Los principales objetivos de esta tesis son desarrollar, implementar y probar una técnica de control factible para el sistema de suspensión activa para la cabina, así como verificar el rendimiento del controlador en términos de reducción de vibraciones y consumo de energía. Este proyecto se centra en el banco de pruebas disponible instalado en ac kth sala de laboratorio el cual simula una cabina real de dicha máquina.

Un estudio exhaustivo de un nuevo prototipo de válvula en el cual se ha testeado el rendimiento de esta válvula bajo diferentes condiciones de uso. Gracias a los test llevados a cabo la válvula pudo optimizarse para que esta trabajara en sus condiciones óptimas en este sistema. Tras la calibración de la válvula un modelo del sistema fue diseñado usando la técnica de la "caja negra". El modelo se aproxima un 96 % al sistema real de la cabina y su comportamiento. Se diseñaron diferentes controladores con este modelo, siendo el que obtuvo el mejor resultado el que se diseñó usando programación de la ganancia.

El sistema tiene un retardo de 36 ms, por lo tanto, se estudió cómo aumentaría el rendimiento de este controlador si se redujera el efecto del retardo. El estudio muestra que la reducción del retardo a valores próximos a 0-2 ms supondría una mejora en el rendimiento de amortiguación de 60 % a 90 %. Smith Predictor se implementó en el controlador de programación de ganancia con el fin de reducir el efecto del retardo. Los resultados demostraron mayor rendimiento y un comportamiento más robusto del controlador con Smith Predictor.

Varios test fueron implementados para obtener diferentes posibilidades que una máquina de este tipo podría encontrarse durante un día de trabajo. Estas pruebas se han realizado tanto en una plataforma de prueba como en un entorno de simulación. La prueba final se realizó utilizando un modelo de una pista de pruebas real de Skogforsk. Esta pista se utiliza para probar diferente maquinaria forestal ya que simula el terreno en un bosque. En base al resultado de la simulación, el porcentaje medio de reducción de las vibraciones del controlador con Smith Predictor es del 70 % lo que muestra que el sistema reduce la vibración de la cabina de una manera efectiva. Además, la potencia máxima necesaria durante la operación del sistema es de 11,63 kW, lo que es factible para implementar este sistema en una máquina real.

Palabras clave: forwarder, suspensión activa, programación de ganancia, Predictor Smith

Contents

Part I

Report

List of Figures

List of Tables

Abbreviations

3D Three Dimensional

CAD Computer-Aided Design

CAN Controller Area Network

CPU Control Programming Unit

ECU Electronic Control Unit

EU European Union

FSA Finite-Spectrum Assignment

IMU Inertial Measurement Unit

KTH Royal Institute of Technology

LTI Linear Time-Invariant

MISO Multiple Input Single Output

MPC Model Predictive Control

MSP Modified Smith Predictor

PC Personal Computer

PCB Printed Circuit Board

PID Proportional-Integral-Derivative

SISO Single Input Single Output

SP Smith Predictor

VSCS Variable Structure Control Systems

VSS Variable Structure System

Table of Contents

1 Introduction

1.1 Background

One of the main industries in Sweden is the forest industry. Sweden has around 55% of forest area and this is why great research and development in this sector is necessary in order to achieve more efficient and economic processes. Nordic Forestry OEMs are a pioneer in the area of mechanized logging which provides forest machines, such as forwarders and harvesters to global customers.

Figure 1: Forwarder machine

A forwarder (Figure 1 [1]) is a forestry vehicle that carries big felled logs which are cut and processed by the harvester. Due to the uneven and rough ground in the forest, operators in the forwarder cab will suffer from whole-body vibration. The ride of heavy machines, tractors, forestry vehicles over a rough terrain leads to cyclic tilting of the machines, which can be regarded as low-frequency (up to several hertz) and high-amplitude (about 10 degrees) vibration of the machine [2]. Studies of truck drivers found that occupational exposure to whole-body vibration could have contributed to a number of circulatory, bowel, respiratory, muscular and back disorders [3]. Therefore, a system which improves the work conditions of the operator is not only needed for health reasons, but also for productivity reasons.

With a passion for technology and responsibility to improve customer experience, Nordic Forestry OEMs are striving for a better driving condition for the forwarder driver. Since vibration in the cab directly influences the driving experience and health of the driver, Nordic Forestry OEMs are dedicated to reduce the vibration in the cab by investigating the feasibility to install an active cab suspension system on the forwarder.

Compared to conventional passive suspension technique, active suspension performs more effectively in the case of low-frequency vibrations [2]. In this project, a forwarder cab rig, including four hydraulic actuators on each four corners, and a Stewart platform which can be used to simulate the disturbance are installed in the KTH lab hall.

1.2 Purpose

This project was inherited from previous project [4]. The hardware used was already done so there was not possibility to modify any of its components. Therefore, one of the main goals is to see how well the active cab suspension can be done on the actual system without major changes on the actual hardware. This project is focused on the controller design of the active cab suspension system. Different control strategies are studied and applied in order to find a controller that optimizes the active cab suspension problem. Not only the control strategy, but also the total power consumption by the system have been studied. No matter how good the system could be in terms of vibration reduction, if it consumes too much power, it will be non-viable to be applied in a forwarder as it would decrease the operating hours of the machine.

The research question for this project can be stated as: *What controller can be designed and implemented on an active suspension test rig in order to reduce vibrations on a forwarder cab and how much power the control strategy requires ?*

In order to be able to answer the research question, different sub-goals were set as a way of guidance:

- Understand the solutions proposed by other researches in the same field. For doing so, a deep literature study needs to be done.
- Check the hardware and solve possible mechanical problems. Adapt the hardware to the requirements of the project.
- Try to optimize the hardware as much as possible to get the best performance out of it.
- Create a model of the system.
- Implement a controller for the model of the system. Once it achieves the desired performance, an implementation of the controller has to be done on the physical system.
- Study how much power the system consumes while the test rig is being operated with the designed controller.

1.3 Scope and Delimitations

The delimitations on the project are presented here:

- This project only considers cab suspension of a forwarder, and it will not focus on any other kinds of vehicles.
- This project is focused on the available mechanical rig installed at KTH lab hall, instead of a real forwarder.
- Vibration reduction is the main aspect considered to verify the model and control performance, instead of other aspects, e.g. energy efficiency.

- Four hydraulic valves and four hydraulic cylinders with integrated position sensors are used.
- dSPACE MicroAutoBox II [5] is used as a control unit hardware.

Additionally, the scope is limited by time restrictions.

1.4 Method

The scientific methods that have been used in this project are simulation and experimental verification. A new model was developed for the system. Therefore, simulation and experimental verification is fundamental since the model has to be a fair representation of the real system.

1.5 Ethics and Sustainability

The active cab suspension is a system in favor of the persons who operate the forwarder. The forwarder operators spend many hours in the machine, and the vibrations can harm their health. It is scientifically proven that long exposure to vibrations can lead to severe back problems. Moreover, large and constant vibrations can decrease the operators' eyesight. These problems can affect the life of the operators and deprive them of having a normal life. Companies should care about their employees or users who are using their products. Therefore, investing in this suspension system is granting a better life for the operators of these heavy machines.

The vibration depletes the productivity of the operators as well. Whole body constant vibration can decrease the concentration and efficiency of the operator which means that they need more time to finish the daily work. The more time the forwarder is functioning, the more carbon dioxide the forwarder emits to the environment. If the active cab suspension system is applied, the vibration will affect less to the operator's productivity, making them finish the task in less time which is also good for the environment.

Safety requirements should be set for the controller since a malfunction of it during the operation could threaten user security. The controller should be normally implemented in an ECU or embedded system in the machine. Therefore, safety constraints should be established for this ECU in case that an undesired individual hacks or manipulates directly the ECU which could lead to a malfunctioning of the system.

Normally, passive suspension elements deteriorate fast which results in a low efficiency. Therefore, they have to be tested and changed regularly in order to keep a good performance. Meanwhile, hydraulic fluid is another thing that needs to be changed over time when the active suspension system is used. Hydraulic fluid is easy to recycle in contrast to a passive spring and damper. Moreover, hydraulic shield in the hydraulic circuit has to be assured since an oil leakage can destroy the flora and fauna in the forest.

2 Frame of Reference

This chapter explains a general background of various suspension systems. It covers relevant aspects for the realization of this system, such as control strategies and important concerns when designing an active cab suspension.

2.1 Suspension Systems

One of the key issues for forestry forwarder is the higher level of vibrations in the cab than most of other vehicles due to the extremely unpredictable rough terrain. These constant vibrations are harmful to the operator. Therefore, suspension systems play an important role to reduce these disturbances in the cab.

The vehicle suspension systems are normally categorized as passive, semi-active and active systems. The mechanical models of the vehicle systems examined in the present study are shown in Figure 2 [6]. They are known as quarter-car models and they are widely used in automotive engineering due to their simplicity and the qualitatively correct information they provide, at least in the initial design stages [7].

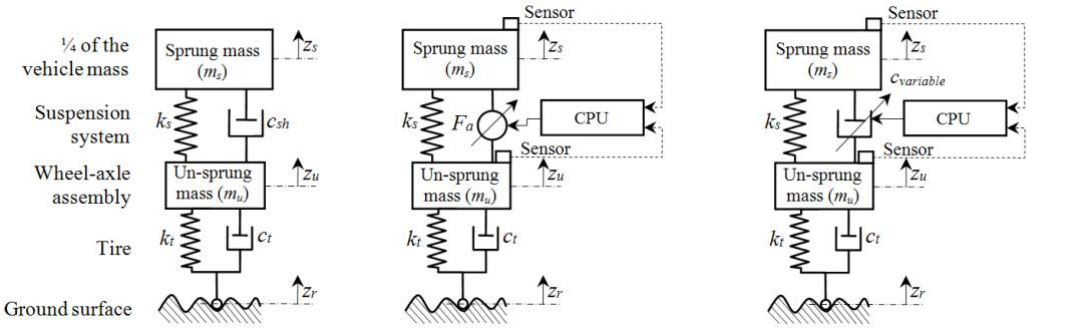

(a) passive suspension (b) active suspension (c) semi-active suspension

Figure 2: Quarter-car models

2.1.1 Passive Suspension

The passive suspension system consists of an energy dissipating element with nonlinear characteristics, which is the damper, and an energy-storing element, which is the spring featuring a linear or nonlinear elasticity [8]. They work mechanically in parallel between the main machine frame (unsprung mass) and the cabin frame (sprung mass), Figure 2a. Since these two elements can not add energy to the system, this kind of suspension systems are called passive.

The characteristics of the springs and dampers are immutable and cannot be adapted to any momentary operational conditions of the vehicle [6]. Thus the vehicle's performance is very limited and any improvements can only be made by the optimization of springs' and dampers' characteristics. Even though these suspension systems do not fulfill all the expectations

regarding comfort and safety, they are widely used due to its low cost, small volume and high reliability.

2.1.2 Active Suspension

An active suspension system, in addition to the already described components, is also comprised of an actuator, sensors, and a control programming unit (CPU), Figure 2b. Actually, the damper is replaced by an active force actuator. The operational conditions of the vehicle are continuously controlled by sensors that measure the velocity of the sprung and un-sprung masses and feeds it to the CPU that ensures correct impulses for the actuator, which creates the desired active damping forces when required [6].

Active suspensions prove to be the most effective approach in the case of low-frequency vibrations (about 5 Hz). In order to handle high-frequency vibrations, passive systems are often added. However handling high-frequency vibrations demands high power consumption by the hydraulic system [2].

2.1.3 Semi-active Suspension

The semi-active suspension system is based on passive and active suspension systems. The semi-active suspension system contains a variable damper instead of a passive one which is automatically controlled by an integrated regulator, Figure 2c. The damping force is modulated in accordance with the operational conditions, which are continuously controlled by sensors connected to the CPU. The correct damping coefficient can be modified by adjusting the orifice area within the damper [6]. Semi-active suspension systems can offer a compromise between the simplicity of passive systems, and the higher performance of active suspension systems. In comparison with an active suspension system, a semi-active suspension requires much less power, and is less complex and more reliable and can provide considerable improvement in vehicle ride quality.

2.2 Efficiency

One of the main concerns in industry and especially in vehicles is efficiency. This is a key point since an efficient system could lead to more operating hours of a vehicle without the need of extra fuel or battery. Therefore, the more efficient the system is, the more hours the forwarder could be working and less the expenses for maintaining the machine. Regarding hydraulic systems, we can find three different types of efficiency: volumetric efficiency, mechanical/hydraulic efficiency and overall efficiency.

The ideal performance of the active cab suspension that could be achieved is damping out all the vibration from the terrain. Nevertheless, for doing so, it might demand a high amount of power which would decrease the operating hours of the forwarder since it would require more energy and more fuel. Hence, it is necessary to find a trade-off point between vibration reduction and energy consumption.

2.3 Vibrations

According to [9], the frequency range that should be taken into account when studying whole-body vibration is from 0.5 Hz to 80 Hz. The vibration in these frequencies could cause disorders and health problems for the vehicle operator. Exposure to whole-body vibration causes motions and forces within the human body that may:

- cause discomfort
- adversely affect performance of the operator
- decrease the efficiency of the operator
- aggravate pre-existing back injuries and
- present a health and safety risk.

As a result, there are not only health problems, but also productivity problems, since the productiveness of the operator may be affected by this vibration, causing lower performance of his/her work.

Machine vibrations are induced by the drives' action, movements of the equipment, variable loading and machine ride. The ride of heavy machine, tractors, forestry vehicles over a rough terrain leads to cyclic tilting of the machines, which can be regarded as low-frequency (up to several hertz) and high amplitude vibration of the machine. The angular motions of the frame are transmitted onto the cab, and the higher the cab position, the larger the amplitude range of linear vibration [10]. According to [11], range of vibration values for forwarders on the EU market is mainly from 0.6 to 1 m/s^2.

2.4 Control Strategies

Hydraulic actuators are inherently velocity sources which means that given a control flow rate into the actuator, a certain velocity is obtained. Therefore, velocity control is rather easy, since the hydraulic actuators normally have precise position sensors. However, hydraulic force control is associated with many problems. The force control is sensitive to different disturbances inside the actuator like friction, stick-slip, breakaway forces, and etc., making force a difficult quantity to control [12]. Thus, most of the existing solutions use velocity and/or position control combined with force control.

2.4.1 Sliding Mode

Sliding Mode control is a particular type of Variable Structure System (VSS) which is characterized by a number of feedback control laws and a decision rule. The decision rule, termed the switching function, has some measurements of the current system behavior as its input and produces as an output the particular feedback controller which should be used at that instant in

time. In sliding mode control, Variable Structure Control Systems (VSCS) are designed to drive and then constrain the system state to lie within a neighborhood of the switching function. A disadvantage of the method has been the necessity to implement a discontinuous control signal which, in theoretical terms, must switch with infinite frequency to provide total rejection of uncertainty [13].

In the article [14], sliding mode control is used for solving the problem of an active suspension with nonlinear actuator dynamics. The reasons of choosing this method are both the robustness and the possibility of creating controller and observer, avoiding the necessity of using more than one method. The results are based on the simulation of a quarter-car model. The model is divided into a linear model (suspension) and a nonlinear one (actuator) in order to decrease the degree of complexity. The results reveal that the controller is able to achieve high precision, fast convergence and strong robustness.

2.4.2 Skyhook

The Skyhook approach was first introduced by Davis Karnopp in 1974 [15]. It is based on using global inertia reference system. The basic idea is to modify the simple structure of a passive system as shown in Figure 3a, moving the damper or adding a damper that is connected to an inertial reference. This method is normally called *sky* as shown in Figure 3b, and as a way of suppressing the vibratory motion of the sprung mass and a tool to compute the desired damping force. From this idea, several control strategies have been developed.

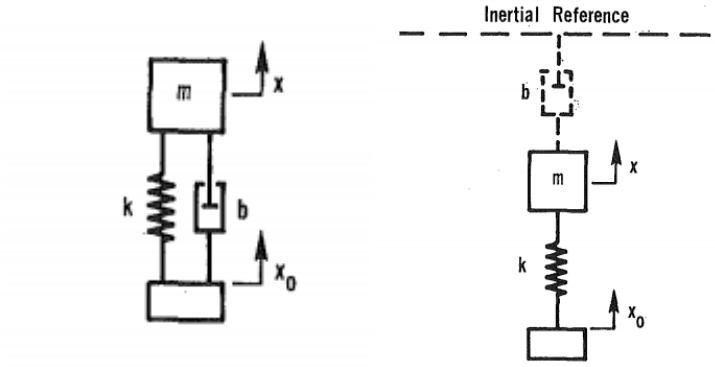

(a) General passive suspension configuration

(b) Skyhook suspension configuration

Figure 3: Configuration comparison

According to [16], skyhook control is an on-off control strategy which changes the damping factor from soft to firm, or vice versa. This change in the damping factor can be simulated as an active actuator which applies the desired force at each moment. The control law for this on-off

skyhook strategy, which defines the force to apply, is

$$f = \begin{cases} -B_1 \dot{x}_1, & \dot{x}_1(\dot{x}_1 - \dot{x}_2) \geq 0 \\ -B_2 \dot{x}_1, & \dot{x}_1(\dot{x}_1 - \dot{x}_2) < 0 \end{cases} \tag{1}$$

where B_1 and B_2 are determined experimentally. The parameters $\dot{x}_1$ and $\dot{x}_2$ are the velocities of the unsprung and sprung masses respectively.

In [17], a control system is designed for an active suspension of a car. The control strategy followed is a combination of different control methods. Figure 4 explains the structure of this method where the controller is designed in a cascade structure with three different loops. The outer feedback loop is designed for the position control. Meanwhile, the other two inner loops are designed for the force control. One of them applies the Skyhook formulas in Equation (1). The other force feedback directly takes the output force from the actuator.

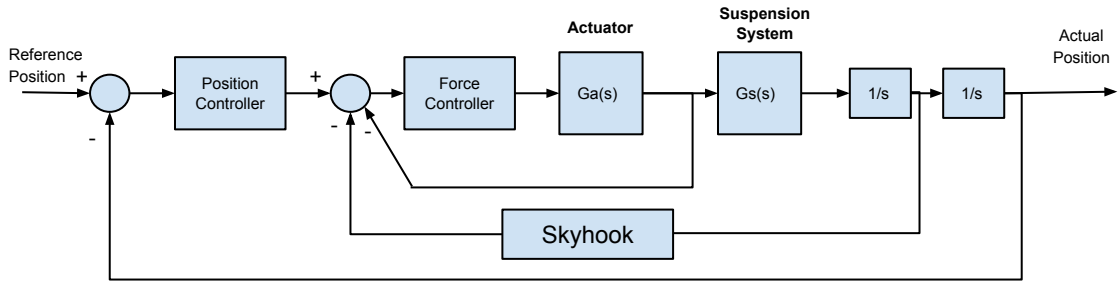

Figure 4: Skyhook control block diagram

2.4.3 Fuzzy Logic

Fuzzy logic control is able to cope with high nonlinear dynamics of systems, since it is based on a decision matrix. A basic Fuzzy controller has the following components [18]:

- Fuzzification interface: The function of this component is to measure the input data and scale it in order to be interpreted by the fuzzy logic. These scaled data sets are called fuzzy sets.
- Fuzzy control rule base: In this stage, control rules are designed in a way to fulfill the control goals.
- Decision-making logic (decision matrix): This component of the fuzzy controller can be interpreted as a decision matrix, since it tries to simulate the decision made by a human. The decision is based on the rules defined in the fuzzy control rule base stage and the fuzzy sets.
- Defuzzification interface: Finally, the output value of the controller is scaled in a way that the system can interpret. In other words, it is the inverse process of Fuzzification.

This type of control strategy has been applied to an active suspension system in [19], manifesting a satisfactory performance. Figure 5 introduces a control block diagram for Fuzzy control.

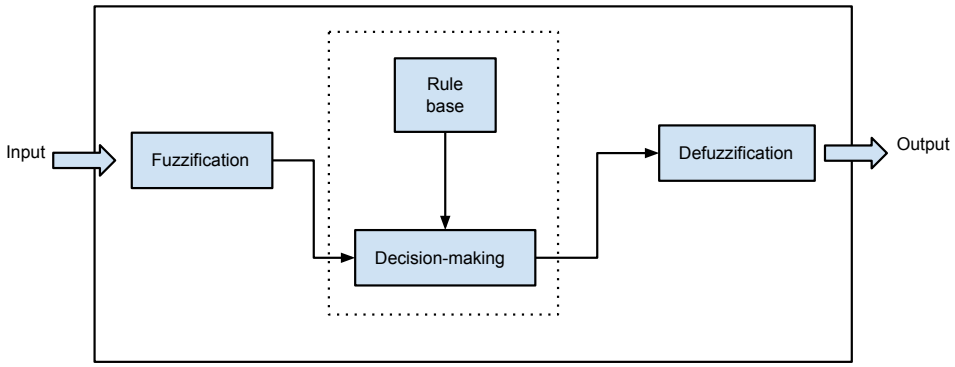

Figure 5: Fuzzy control block diagram

2.4.4 Gain Scheduling

The gain scheduling approach is perhaps one of the most popular nonlinear control design approaches. It has been widely and successfully applied in fields ranging from aerospace to process control [20]. Because of cost considerations and performance requirements, gain scheduling techniques were employed in military applications relatively early, while commercial applications of gain scheduling began when digital computer control became available. In other words, gain scheduling is an old idea, but before digital implementation of controllers, it was expensive and difficult to realize on hardware.

A number of aspects of gain scheduling are listed below [21]:

- Gain scheduling employs powerful linear design tools on difficult nonlinear problems.
- Most performance specifications are phrased in linear terms, involving a mixture of time-domain and frequency-domain specifications.
- Gain scheduling does not require severe structural assumptions on the plant model. The approach can be used in the absence of complete and analytical plant models.
- Design by gain scheduling preserves well-understood linear intuition and it is carried out using the physical variables in the plant model.
- Gain scheduling design approaches are naturally compatible with decompositions of the overall control problem.
- Gain scheduling enables a controller to respond rapidly to changing operating conditions. For this it is important that the selected scheduling variables reflect changes in plant dynamics as operating conditions change.

- The computational burden of linearization scheduling approaches is often much less than for other nonlinear design approaches.
- The linearization scheduling approach does not apply when little information is carried by plant linearizations about constant equilibria.
- Linearization gain scheduling depends on intuitive rules of thumb and extensive simulation for evaluating its stability and performance. Typically, stability can be assured only locally and in a "slow-variation" setting.

Generally, the core idea of the gain scheduling is continuously varying the controller coefficients according to the current value of scheduling signals, also called scheduling variables, which may be either exogenous or endogenous signals with respect to the plant [21].

In broad terms, the design of a gain scheduled controller for a nonlinear plant can be described as three steps [22]:

- In the first step, a set of equilibrium points, also called operating points, are selected. The most common approach is based on Jacobian linearization of the nonlinear plant over a set of operating points. Next, a linear time-invariant (LTI) or time-varying description of the nonlinear system is derived for each selected operating point. As a result, a family of LTI models parametrized by the scheduling variables are obtained.
- The next step is designing an LTI controller for each member of the family, so that stability and performance are guaranteed at the corresponding operating point. Any available tool for linear control design can be used in this step.
- The third step is the planning of the gain scheduling, i.e., the formulation of an algorithm that modifies the controller according to the value of the scheduling variables.

In order to describe this method mathematically, considering the plant dynamics are described by nonlinear differential equations of the form [23]

$$\begin{aligned} \dot{x} &= f(x, u, \sigma) \\ y &= g(x, u, \sigma) \end{aligned} \tag{2}$$

where x is the state vector, u is the plant input, and σ is the scheduling variable. These equations can be specified explicitly or implicitly, such as by a Simulink model. For nonlinear plants, the linearized dynamics describe the local behavior of the plant around a family of operating points $(x(\sigma), u(\sigma))$ parametrized by the scheduling variables, σ. Specifically, the deviation from nominal operating condition are defined as

$$\delta x = x - x(\sigma), \quad \delta u = u - u(\sigma) \tag{3}$$

These deviations are governed, to first order as

$$\dot{\delta x} = A(\sigma)\delta x + B(\sigma)\delta u, \quad \delta y = C(\sigma)\delta x + D(\sigma)\delta u \tag{4}$$

$$
\begin{aligned}
A(\sigma) &= \frac{\sigma f}{\sigma x}(x(\sigma), u(\sigma)) \qquad B(\sigma) = \frac{\sigma f}{\sigma u}(x(\sigma), u(\sigma)) \\
C(\sigma) &= \frac{\sigma g}{\sigma x}(x(\sigma), u(\sigma)) \qquad D(\sigma) = \frac{\sigma g}{\sigma u}(x(\sigma), u(\sigma))
\end{aligned} \tag{5}
$$

When repeated for a finite set of design points, σ, this local linearization produces a series of LTI models.

2.4.5 Model Predictive Control

Model Predictive Control (MPC) originated from late seventies and has developed considerably since then. The term Model Predictive Control does not designate a specific control strategy but rather an ample range of control methods which make explicit use of a model of the process to obtain the control signal by minimizing an objective function. The key of MPC is to use the model as a reference point and, in real time, calculate multiple paths that can be taken by assigning different values for the manipulated variables and look at the system model response. An algorithm is implemented that goes through the different paths and chooses the control action which is closest to the desired outcome within a specified time interval. MPC has already been developed and accepted by the academic world and industry. There are many successful application examples of MPC which prove good performance and capacity of MPC to achieve efficient controllers [24].

In broad terms, the approach of MPC can be described as the general steps, represented as follows [25]:

- Create a very accurate model of the system and set desired constraints and rules for the system.
- At time t (initial condition) compute a number of future outputs $y(t+k|t), k = 1 \cdots N$. They depend on future inputs $u(t+k|t), k = 0 \cdots N-1$ and on measurements known at time t.
- The set of future control signals is calculated by optimizing a determined criterion to keep the process as close as possible to the reference trajectory.
- Apply $u(t)$ to the physical plant.
- Wait for the next sampling instant $t+1$ and repeat step 1.

One of its advantages is the availability to be used to control a great variety of processes, from those with relatively simple dynamics to more complex ones, including systems with long time-delay or non-minimum phase or unstable ones. However, the biggest risk of this method is the discrepancy between the plant and the model which is used for designing the controller [24].

2.5 Delay

For real time application such as the active suspension, a delay in the system affects on the final performance of the system. In order to reduce the effect that the delay produces in the system, the following methods could be applied [26].

2.5.1 Smith Predictor (SP)

The Smith Predictor was proposed in order to design a controller for a time-delay system so that the delay is shifted outside the feedback loop. Therefore, it makes the control design and system analysis simplified and reduces the negative effect brought by the time-delay. This is realized by introducing a local feedback to the main controller $C(s)$ by using the Smith Predictor $Z(s)$, as shown in Figure 6 [26]. The plant $G(s) = P(s)e^{-sh}$ is assumed to be stable and the Smith Predictor

$$Z(s) = P(s) - P(s)e^{-sh} \tag{6}$$

is implemented using models of the delay-free part P(s) of the plant, and the plant $P(s)e^{-sh}$.

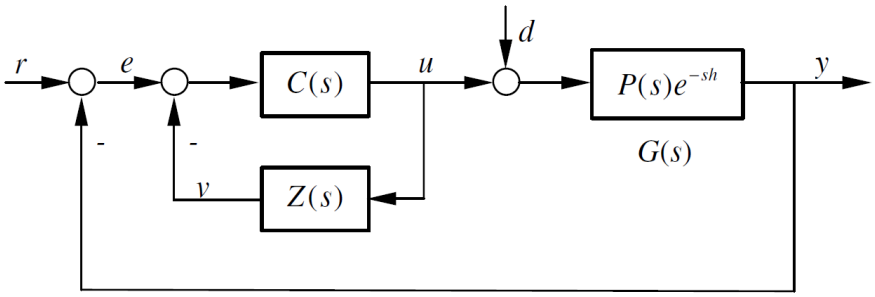

Figure 6: Smith Predictor control system

Assume that $d = 0$ and there is no modelling error, then the inner loop can be replaced by

$$C'(s) = \frac{C(s)}{1 + C(s)P(s)(1 - e^{-sh})} \tag{7}$$

where $C'(s)$ can be seen as a compensation controller. Then the closed loop transfer function of the system is

$$\Phi(s) = \frac{C'(s)P(s)}{1 + C'(s)P(s)} = \frac{C(s)P(s)}{1 + C(s)P(s)}e^{-sh} \tag{8}$$

In this case, the system is equivalently shown in Figure 7 [26], which shows that the delay is moved outside the feedback loop and the main controller $C(s)$ can be designed according to the delay free part $P(s)$ of the plant only. Although the gain constraint on the controller is reduced, it still has to be a compromise between the robustness and the speed of the system.

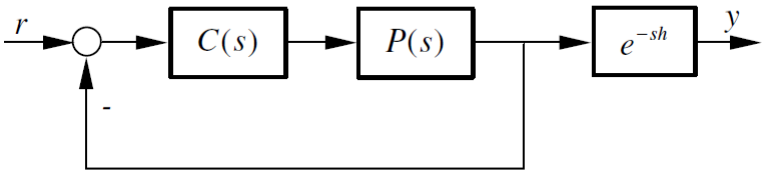

Figure 7: Smith Predictor simplified control system

2.5.2 Modified Smith Predictor (MSP)

As its name implies, it is a modification of the classic Smith Predictor method. This modification allows to control the time delay in systems which are not stable [26].

2.5.3 Finite-Spectrum Assignment (FSA)

The SP-based control scheme is very effective for control of stable time-delay systems, while the modified Smith Predictor was being developed for unstable systems. Another effective control strategy, known as finite-spectrum assignment, was developed for unstable systems as well. This strategy can address delays not only in the input/output channel, but also in the states [26].

3 System Overview

In this chapter, the elements constituting the system are discussed in terms of hardware preparation, communication setup and operation modes selection.

3.1 Physical System

In this project, an actual mechanical structure (test rig) of a forwarder is utilized for the research on the active cab suspension. The functionality of this element is to connect the cab with the main structure of the forwarder. Figure 8 [27] represents a 3D model of test rig.

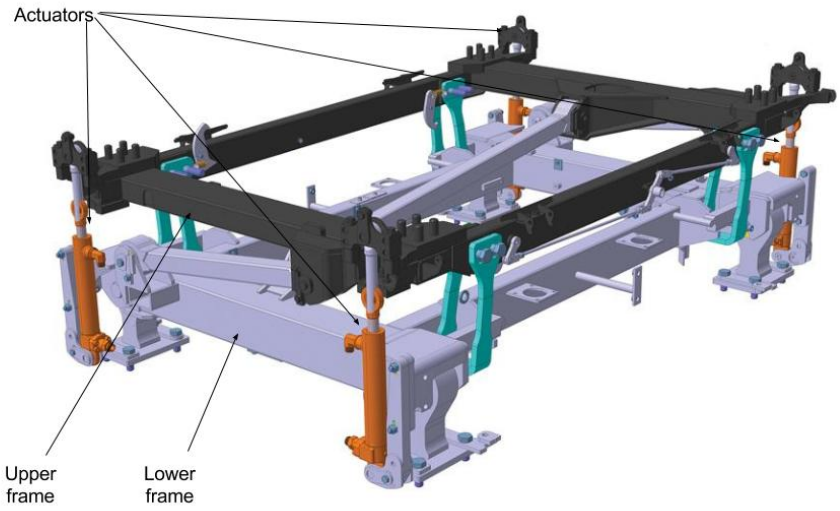

Figure 8: 3D model physical structure

The test rig does not have a cab on top of it. It is formed by two different frames that are independent of each other. The joint points between them are four hydraulic actuators, one on each corner of the rig. These actuators are used to compensate the disturbances coming from the lower frame to the upper frame. The actuators are governed by 4 hydraulic valves (one for each actuator). However, the valves are designed for heavy load cranes. Therefore, it is very challenging to adapt these valves to an active cab suspension system, since the load of the cab is rather small (1 ton). Figure 9 [4] introduces the real test rig, and its main components are labeled by different numbers. Number 1 to 4 correspond to the 4 actuators, number 5 and 6 represent the lower and upper frame respectively.

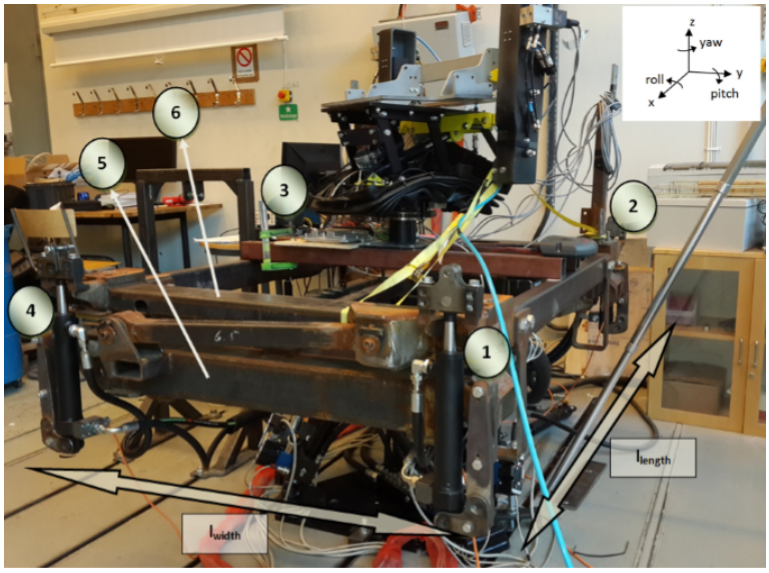

Figure 9: Real physical system

The hydraulic valves are fed by Parker PV063 axial piston variable displacement pump with approximately 100 L/min flow capacity and fixed 170 bar pressure.

3.2 Hydraulic Valve

The valve has two spools, P Spool and T Spool. These two spools are independent of each other. P Spool is the one that connects the ports of the valve, A and B, with the pump. T Spool has the same function as P spool but it connects the ports with the tank instead of the pump. P Spool connects B port with the pump for positive values of the P spool and T Spool connects port A with the tank for positive values of the T spool. Applying negative values to the two spools changes the roles, A port is connected with the pump and B port with the tank. Both spool positions must have the same sign, either positive or negative. The voice coil applies a current for moving the spools. The higher the current, the higher speed at which the spools move. The ports of the valve are connected to the actuator. A port is connected to the actuator piston side and B port is connected to the actuator rod side.

3.3 Sensors

A set of sensors is distributed around the test rig in order to gather the necessary data. It is formed by:

- IMU: It is placed on the lower frame and used to monitor the motion of the lower frame.
- Four position sensors: One for each actuator.
- Valve pressure sensors: The valve has integrated sensors for measuring A port, B port, tank and pump pressures.

- Valve spool position sensors.

3.4 Communication

The first attempt was continuing with the same communication structure that was already implemented as summarized in Figure 10 [4]. This implementation was using a NI cRIO-9076 hardware system from National Instruments and two extra modules NI-9853 and NI-9203 which basically are a CAN module and an analog input module.

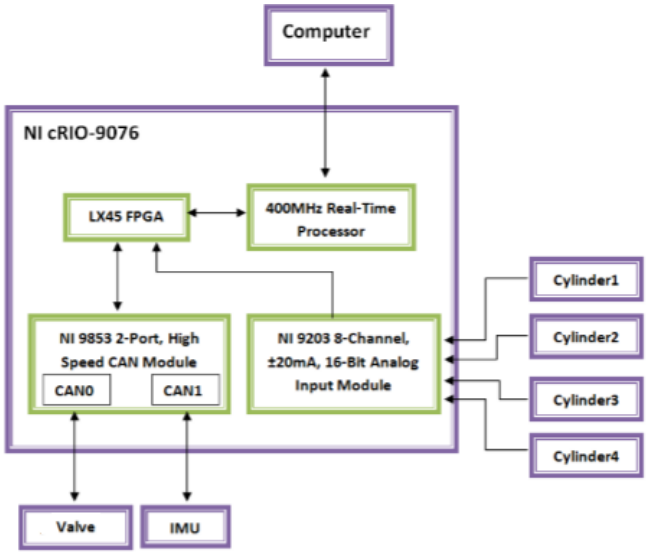

Figure 10: First communication layout

However, for the realization of this project, it was decided to use dSPACE hardware instead of National Instruments, since the authors have a better understanding of it and its seamless integration with Simulink. Moreover, new functionalities have been included that were not possible to be achieved by NI cRIO-9076, such as that more CAN channels are required at different baud rates. The hardware finally used in this project is dSPACE MicroAutoBox II. From now on, it is mentioned as control box.

Starting from the position sensor, it is connected directly to the control box. The output of the sensor is a current signal 4-20 mA. The control box has four analog inputs in form of voltage. Therefore, a converter PCB board was made for converting current to voltage. The PCB board integrates passive low pass filters as well.

The IMU communicates with the control box through CAN with a baud rate of 500 Kb/s. The valves communicate with the control box via CAN as well. There are two different CAN channels in the valves, internal CAN and external CAN. The external CAN is used for the communication between the valves and the exterior (user). Meanwhile, the internal CAN is used for the communication between valves. However, this internal CAN can be accessed from an external computer, which gives great convenience for the control. The sensor measurements

have more resolution when the data is read from the internal CAN. Moreover, the sampling and transmission speed is faster in the internal CAN than the external CAN. External CAN has a baud rate of 250 Kb/s. In contrast, the internal CAN works at 1 Mb/s of baud rate.

Finally, the control box is connected to a PC where Simulink and MATLAB are used to program and as user interface. Figure 11 depicts the new communication layout.

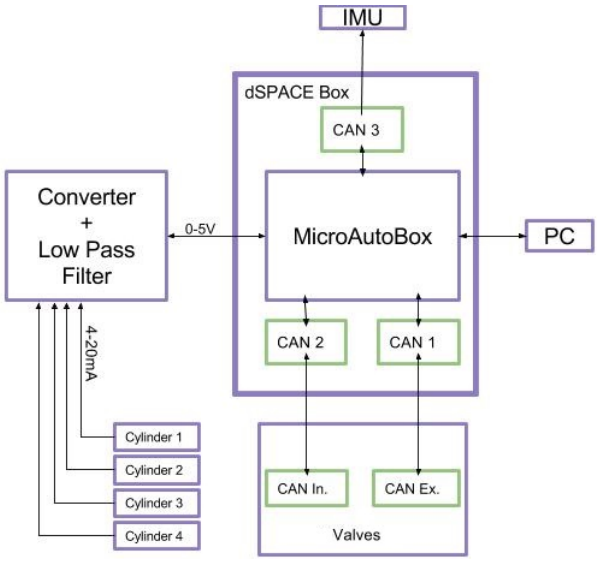

Figure 11: Final communication layout

3.5 Valve Operation Modes

The valves have a wide range of modes that can be selected according to the application and operation conditions of the valves. These valves have a large amount of parameters that can be modified in order to adapt the behavior to the desired one. This section explains the modes that have been studied for this project. The rest of the modes are not of interest for our application.

3.5.1 Flow Control

In this mode, the reference signal is a flow command that is sent via CAN bus. The internal controller of the valve sets the spools position according to the input command. Inside the flow control mode, there are several sub-modes that modify the response of the valve. The sub-modes studied are explained below.

Meter In and Meter Out In these modes, the valve conducts flow control from pump to the load (meter-in flow) or from the load to the tank (meter-out flow). Therefore, with this operation mode, the flow is controlled either from the pump to the actuator or from the actuator to the tank but not both at the same time. This is not desired for an active suspension system, since the response of extending and retracting the cylinder is different.

Flow In/Out A port (Pressure Control on B port) In this mode, the valve conducts flow control from pump to A port and conducts flow control from A port to tank (depending on the sign of the flow set point). This mode is a combination of the Meter In and Meter Out which is applied to the port A.

Flow In/Out B port (Pressure Control on A port) It has same behavior as the previous mode, but the control of the flow is applied in the port B in this case.

3.5.2 Spool Position Control

This mode gives more freedom, control wise, since the spool position of the valve is used as input command. In this case, two messages are sent via CAN, one for each spool. In this mode, the controller for the spool position is already implemented in the valve. There is possibility of tuning this PID controller (Kp, Ki and Kd) in order to change the response and behavior of the spool.

3.5.3 Current Control

This is the most inner loop for controlling the valve. In this mode, the input is the current for the voice coil which steers the spool and there is not any controller implemented for the spool position. If this mode is used, a spool position controller must be designed.

3.6 System Limitation

Since the system is not a real forwarder active cab suspension, it has some limitations that are necessary to deal with. The dimensions of both upper and lower frames are 1.85 m length and 1.05 m width, and the actuators have a stroke of 20 cm. Therefore, the physical constraints in terms of freely movement of the upper frame are 20 cm for heave, 5° for pitch and 9.5° for roll.

The test rig used in this project does not have a real cab on top of it. This means that it is not operating at the same conditions as it would be in the real situation. Hence, the results obtained in this system might differ from the ones that would have been obtained in the actual suspension system of the machine. Loading the test rig with more weight was not possible due to two factors. Firstly, there was another project conducted on top of the upper frame, so it was difficult to put load on the rig, since it might affect the other project work. Secondly, the Steward platform has a load limitation of 1 ton. The total weight already on the platform is around 600-700 kg, so the maximum load that would be possible to put on is around 300 kg. This amount of load is far from the normal weight of an actual forwarder cab. Therefore, it was decided not to use an extra load in this project.

One of the main limitations of the system is the valves. They were already on the system and it was not possible to use other types. These valves are not designed for this application, instead they are designed for cranes and for the movement of big loads. In this project, it is necessary

for the valves to have a fast response and high precision. However, these valves have a slow response to the input and big deadbands in the spools. Moreover, they are prototypes which have some weak points such as the pilot springs which move the spools. Due to the constantly moving of the spool while controlling the valves, some of these springs could not handle the stress and broke down, which slowed the project, because the rig could not be used until valve replacements were received.

4 Implementation

This chapter describes how the implementation was realized. It explains how the hardware was set up for the correct functioning of the system. The model identification is discussed including all the steps and attempts followed. Through this model, different control approaches were developed for designing a controller of the active cab suspension system.

4.1 Calibration of the Sensors

The sensors are critical for the system and they need to be well calibrated in order to have a reliable measurement. The only sensors that are possible to have access for tuning them are the position sensors. The valve sensors are supposed to be already calibrated and ready to be used.

The first step was converting the current output signal from the position sensor into voltage, since the MicroAutoBox II just accepts 0-5 V input instead of current. As a result, a PCB was designed and made. The function of the PCB board is converting the current to an acceptable value of voltage as well as powering the position sensors with 24 V. The PCB board also includes passive low pass filter with cutoff frequency of 5 Hz. It is mounted in a suitable box for avoiding harm in use. The distance between the position sensor and the MicroAutoBox II is around 5 m. Therefore, it was decided to place this box as close as possible to the MicroAutoBox II, since a voltage signal is more sensitive to noise than a current signal.

The position signal measured from the box is quite noiseless and it can be used directly without any other digital filter. However, the noise effect increases when the velocity is derived from the position. In order to solve this problem, different digital filters were tested. The first attempt was using a Butterworth filter with a cutoff frequency of 3 Hz. The output signal after the filter was smoother than the raw signal. On the other hand, compared with the raw signal, the filtered signal has a considerable phase lag and a part of the fast velocity dynamics are lost. The next choice was using a Kalman filter. The signal after filtering is less smooth than Butterworth filters, but the dynamics of the velocity is not lost and the lag is much less. Figure 12 shows the comparison between both filters as mentioned above. As a result, the velocity response using Kalman filter is much faster and is able to record the first velocity peak after sending an input in open loop. Therefore, the Kalman filter is used in the final solution of this project

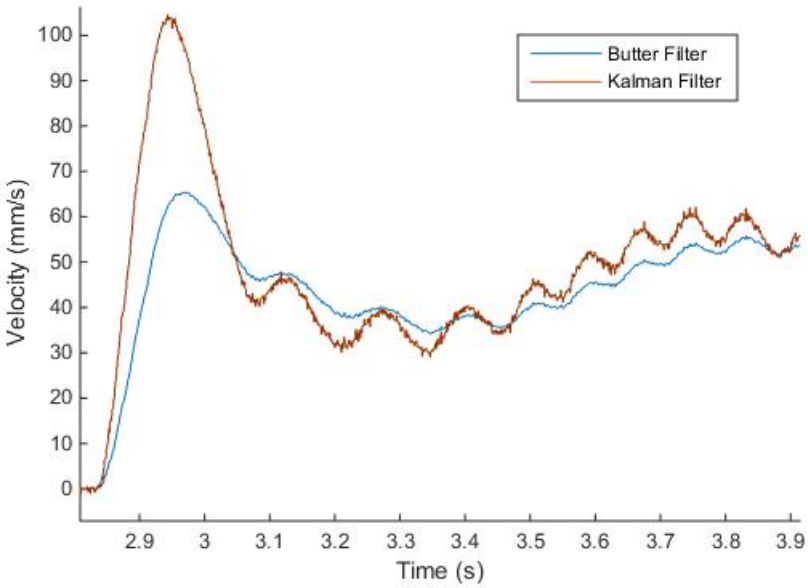

Figure 12: Kalman and Butterworth filter comparison

4.2 Valve mode selection

This section discusses the different tests conducted in order to compare different valve modes described in Section 3.5. The comparisons are mainly focused on the delay between input and output as well as the behavior of the valve. Finally, a conclusion is made based on the results of the tests.

4.2.1 Flow Mode

The mode "Flow In/Out A port (Pressure Control on B port)" outperforms the other modes, since it has similar behavior and velocity in both extension and retraction of the hydraulic actuator.

The test was realized in one single actuator. An input flow command was sent to the valve. The velocity and the response of the actuator was monitored and recorded. Figure 13 reveals the main problem with this mode which is a big delay between the input command and the actuator movement.

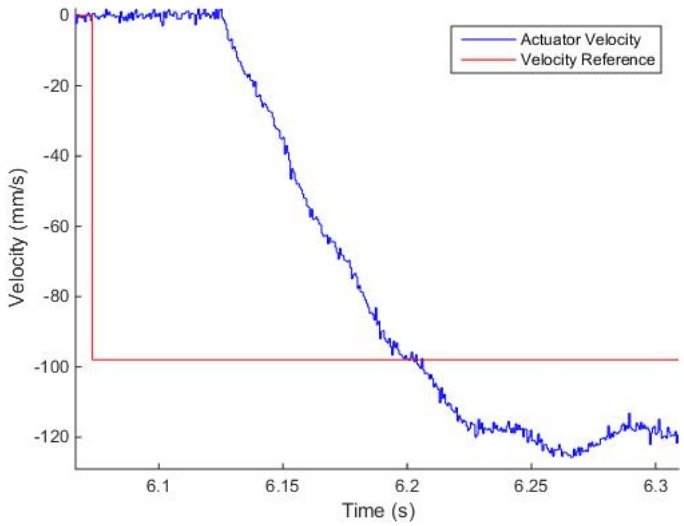

Figure 13: Flow delay

The measured delay is approximately 80 ms. Friction is not the main reason for this phenomenon, since the delay remains constant for different references. It is deemed that the delay results from internal communication and processing in the valve embedded system.

4.2.2 Spool Position Mode

The same procedure as in the flow mode was carried out. A spool position reference set point was sent to one of the spool. The spool position reference and the actual spool position was logged as shown in Figure 14.

From Figure 14, the delay between input and output is around 10-15 ms which is much smaller compared to the previous delay. However, it was noticed that the movement of the actuators did not start until around 36 ms. It is due to a deadband that the valve has. Each spool has a deadband of 1.5 mm in both negative and positive direction from the neutral position. So, the spool has to pass the deadband in one direction which takes around an extra 20 ms. Then, if the actuator is moving in one direction and intends to change the movement direction, it has to move the spool around 3.0 mm until passing both deadbands. Figure 15 illustrates that the delay is around 36 ms until a change on the pressure of two ports as well as on the movement of the actuator. Once the reference is sent, the spools start moving after 11 ms. Nevertheless, both the pressure in the two valve ports and the actuator position remain still until the spools reach a position of 1.5 mm. After that moment, the pressures in two ports start to change and the actuators start to move. It has been experimented to change the gains of the PID controller for the spool position in order to make the response of the spool faster and pass the deadband faster. However, the spool behaviour became unstable with big oscillations, revealing the spool position controller has been tuned well as default.

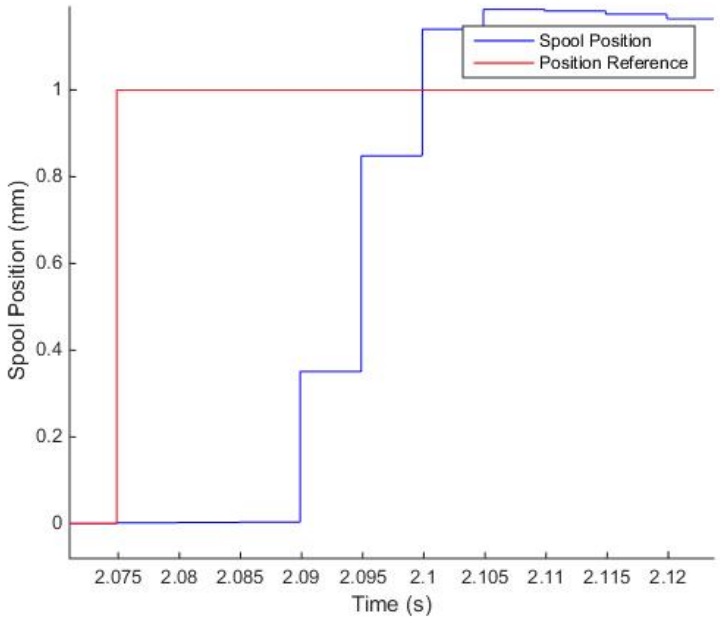

Figure 14: Spool delay

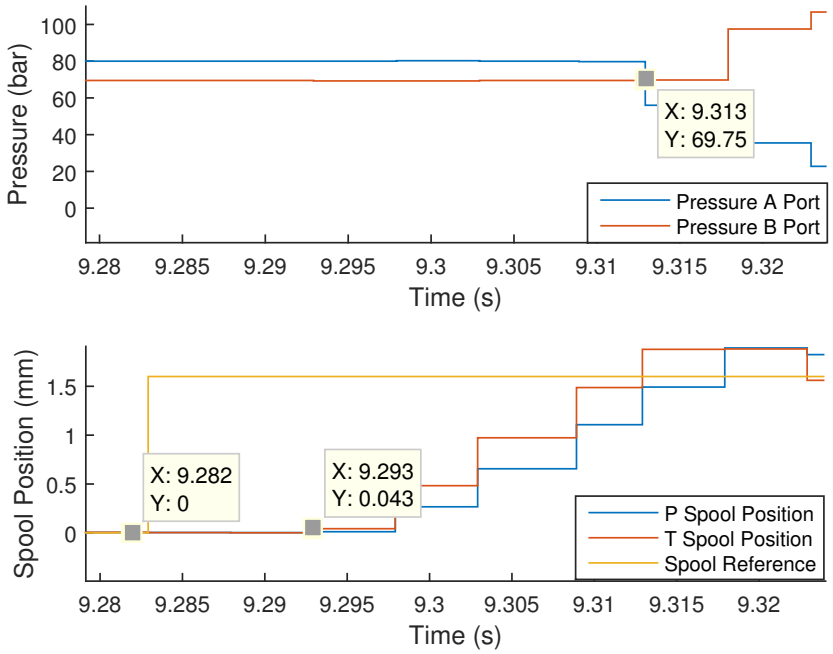

Figure 15: Spool deadband influence

4.2.3 Current Mode

In this case, current for the voice coil that manages the movement of the spool is used as input. In this mode, it is possible to receive a feedback message indicating when the valve has received and stored the current input reference. Figure 16 demonstrates that it only takes 4 ms for receiving and storing the reference command in the embedded system that controls the valve. The oscillation in the current is due to the 50 mA dither current with a frequency of 333 Hz implemented.

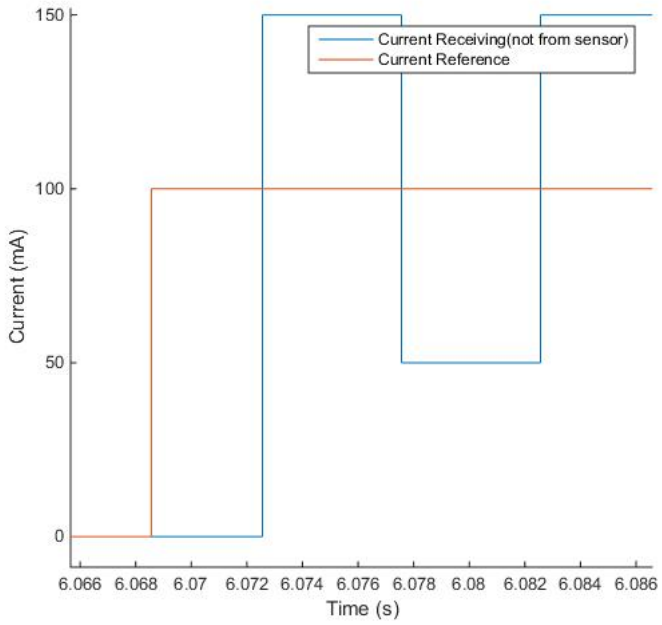

Figure 16: Current communication delay

However, Figure 17 shows that it still takes around 10-15 ms for the spool to start moving. It is interesting to show the plot above since it presents that the delay is originated inside the valve and it is due to processing delay instead of communication delay. It is not caused by friction either, since different references were sent with different amplitudes and it was still 10-15 ms until the spool reacted.

As it was not possible to decrease the processing delay (10-15 ms), a different experiment was performed in order to test if the spool can overcome the deadband in a shorter time. This test is represented in Figure 17 where a current of 600 mA was sent to the valve right after the dash line. This current is the maximum current accepted by the voice coils.

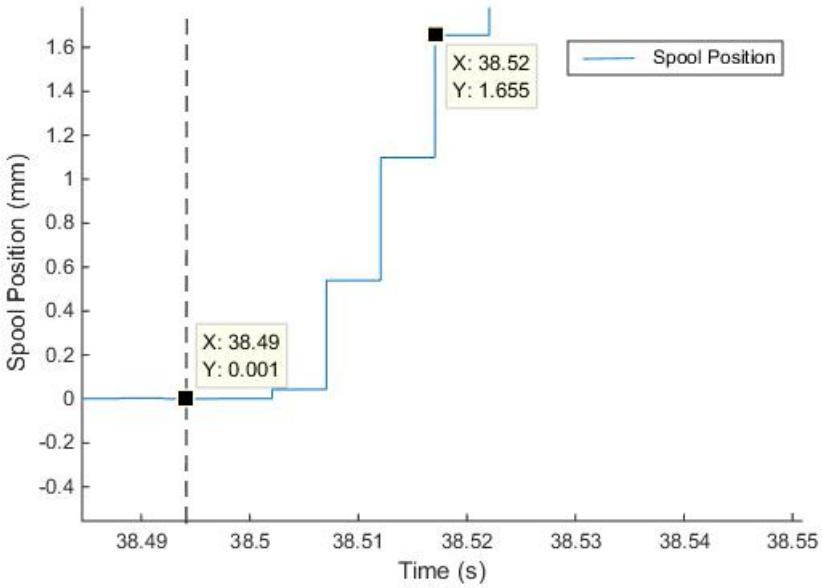

Figure 17: Spool response with maximum current

It shows that the time which the spool takes for overcome the deadband is around 20 ms. If the processing delay of 12 ms is summed with 20 ms, a final delay of 32 ms until the actuator starts moving is obtained.

4.2.4 Conclusion

There are different advantages and disadvantages of the different modes. In the flow mode control, the main advantage is the simplicity. The signal sent to the valve is a flow command, then the valve feeds the desired flow to the system. Moreover, the behavior of this mode is approximately linear which simplifies the system. The spool position and flow controller are already implemented in the valve, which simplifies more the way of solving the problem. However, the big delay encountered in this mode is the significant drawback. Due to the fact that fast response is crucial for the success of this kind of system, this mode has not been chosen for the controller design.

In the case of sending the spool position as the input, the delay was decreased to half. However, this mode is more challenging control wise, because the response of the system is not linear and it requires more specific knowledge about the valve such as the specific opening area coefficient depending on the spool position.

Finally, the performance of the current mode in terms of delay is almost the same as the spool position mode. Both of them take around 30 ms to make the actuator move. Moreover, the current mode did not decrease the deadband effect. Finally, if this mode were selected, a position controller would need to be designed for the spool. In Figure 17, it was shown that even with the maximum control input of 600 mA, the deadband was not passed until 20 ms, which

finally has a delay around 32 ms. Therefore, it would be an extra effort to design a controller for the spool while there is one already implemented in the spool position mode. Moreover, the current sensor in the valve is not well calibrated which is not trustworthy for controller design.

Following the reasoning above, the best mode is the spool position mode, which is selected for the controller design finally.

4.3 Model of the System

Different attempts of the model were made in order to find the best approximation of the real system. In this section, all these models are tested and verified. A detailed explanation and procedure for obtaining these models are described in this section.

4.3.1 Theoretical Model

The first attempt was modifying one spool valve theoretical model into a two spools valve model [28]. These are the constitutive equations for the valve when $Xv_P, Xv_T > 0$:

$$Qv_B = Rv_P(Xv_P) \times \sqrt{p_{pump} - p_B} \tag{9}$$

$$Qv_A = Rv_T(Xv_T) \times \sqrt{p_A - p_{tank}} \tag{10}$$

$$Q_B = Qv_B - Qc_B \tag{11}$$

$$Q_A = -Qv_B + Qc_A \tag{12}$$

These are the constitutive equations for the valve when $Xv_P, Xv_T < 0$:

$$Qv_B = Rv_T(Xv_T) \times \sqrt{p_B - p_{tank}} \tag{13}$$

$$Qv_A = Rv_P(Xv_P) \times \sqrt{p_{pump} - p_A} \tag{14}$$

$$Q_B = -Qv_B + Qc_B \tag{15}$$

$$Q_A = Qv_B - Qc_A \tag{16}$$

Common equations in both directions:

$$Q_B = C_f \times \dot{p}_B \tag{17}$$

$$Q_A = C_f \times \dot{p}_A \tag{18}$$

$$Qc_B = A_{rod} \times v \tag{19}$$

$$Qc_A = A_{piston} \times v \tag{20}$$

where R_P and R_T are the relationships between the spool position and the opening area, and the unit of these factors are $m^3/(sec \times \sqrt{pas})$. These variables are provided by the manufacturer of the valve. p_{pump} and p_{tank} are the actual pressures in the pump and tank respectively. Qv_A and Qv_B are the flows coming in/out of the valve, depending on the spool position. Qc_A and Qc_B are the flows that move inside the actuator piston side (connected to the A port) and rod side (connected to B port) respectively. Q_A and Q_B are the flows into the cylinder seen from A and B port respectively. A_{rod} and A_{piston} are the areas in rod and piston side respectively. v is the velocity of the piston. C_f depends on the volume and the bulk modulus which is supposed to be constant and with a value of $2 \times 10^9 N/m^2$.

This model was implemented in Simulink for one actuator. A Simulink block diagram of the theoretical model is in Part III where Figure 49 shows the block used for both directions of the cylinder (retracting and extending) and in Figure 50 is explained more in detail the retraction block diagram which is similar to the extension but changing some signes. The position of the spool is used as input and the velocity of the piston as output of the system. However, it is difficult to match the behavior of the real system with the model as shown in Figure 18. The problem is identified on the R_P and R_T look up tables provided by the manufacturer. In order to obtain a desirable behaviour of the model and have the right output, it is necessary to add a gain right after the look up table. The problem is that this gain is not constant and if the spool position reference is slightly changed, this gain has to be modified in order to match again the output of both model and real system. Moreover, the valve is a prototype valve, so there is not proper data-sheet and graph that can be used to correct and validate this relationship. In Figure 18, the shape of the two curves are identical but they differ in gain. As mentioned, this gain is not constant when changing the reference. However, the gain calibration requires long time and instruments like a flowmeter which is not available in the system, so it was decided to use another approach.

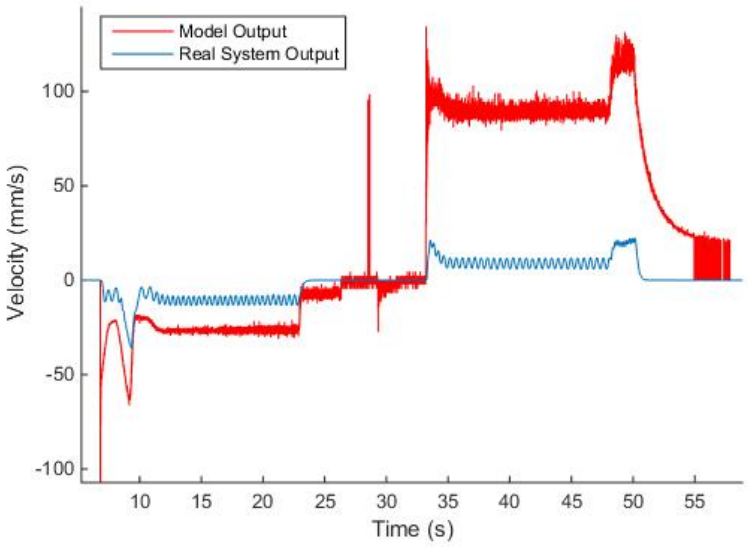

Figure 18: Real system velocity response vs. model velocity response

4.3.2 Black-box Model

Black-box Model is useful for system identification when little information is known. This is the case for this project due to the fact that there is a lot of unknown information about the actual valve. The System Identification toolbox from MATLAB is used for obtaining an approximate model of the system with which a controller can be implemented. With the purpose of simplifying the model, it was supposed that both spools move to same position simultaneously. Proceeding in this way, the system is transformed from Multiple Input Single Output (MISO) to Single Input Single Output (SISO). In brief, the model input is the spool position and the output is the velocity of the actuator. The same model was used for all four actuators. In order to achieve a precise model, a great quantity of input and output data of one actuator has to be recorded for the model estimation. Figure 19 shows the data gathered for the model estimation.

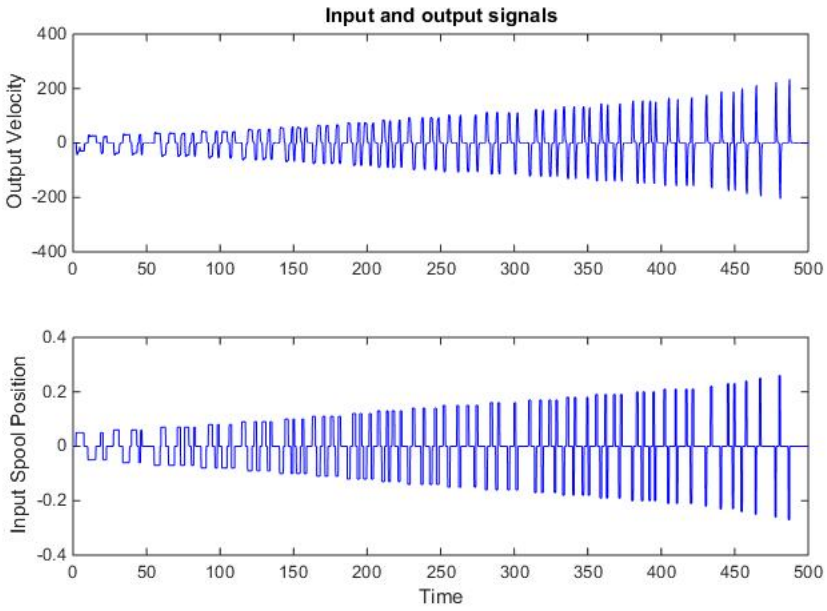

Figure 19: Black-box system identification data

In Figure 19, the relationship between the input command and the output is not linear. Hence, the nonlinear Hammerstein-Wiener structure was used for the approximation of the model. Figure 20 introduces the mentioned structure which is composed of an input non-linearity, a linear block and an output non-linearity. The non-linear blocks consist of two piece-wise linear functions shown in Figure 21 and the linear function is a discrete transfer function of second order with no zero, Figure 22. This structure was used, since it provided an intuitive model.

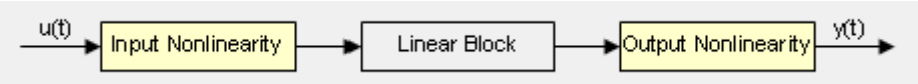

Figure 20: Hammerstein-Wiener structure

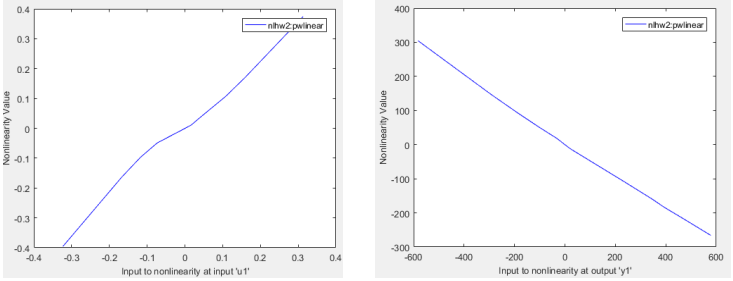

(a) Input Nonlinearity (b) Output Nonlinearity

Figure 21: Piecewise liner input and output of the nonlinearmodel

$$G(z) = \frac{z^{-20}}{1 - 1.919 \times z^{-1} + 0.9193 \times z^{-2}} \tag{21}$$

Figure 22: Discrete transfer function of the linear block

The model estimation was able to match around 96% of the data. Then the model was verified with the real system. Regarding the verification data, one of the three left actuators was used. In other words, the actuator for gathering the data and for verification was not the same. Figure 23 illustrates the verification result.

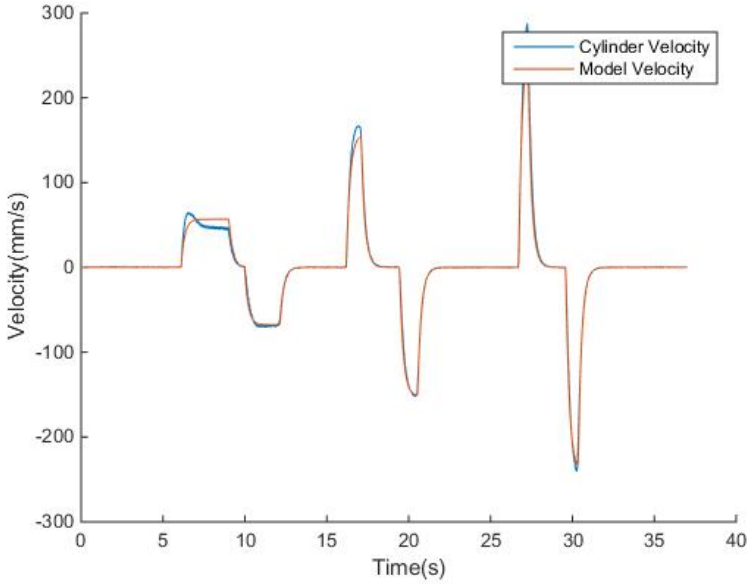

Figure 23: Model verification

Due to the high matching between the model and real system, this model is utilized for the realization of the active cab suspension controller.

4.4 Control

In this section, it is explained the control design process of this project. Before explaining with more detail the solution adopted, it is necessary to comment some limitations and decision regarding the chosen control strategies.

From the different options studied in Section 2.4, two options were implemented: Linear PID controller and Gain Scheduling controller. The author had more knowledge in these two options being possible to obtain a better performance and optimization of the system. Moreover, Gain Scheduling was a potential candidate since from the study of the system dynamics it was concluded that for small regions of the input range, the system could be considered lineal. Regarding Sliding Mode Control and Model Predictive Control were not finally implemented

for both lack of time and less experience with them. Thus, it is proposed to do further work with other control approaches in order to research if there is any other solution which performs better for this system than the one studied. Finally, Skyhook Controller would be a viable option if force is a parameter that can be controlled. Nevertheless, as it was concluded before the theoretical model was not working as expected being not possible to control either force or pressure in the actuators.

The delay is another issue which this project has tried to mitigate using Smith Predictor introduced earlier as well. Since the system is stable, the method used is the simple Smith Predictor.

4.4.1 Control Strategy

In order to design the suspension system, it was considered that the movements of the actuators are independent and they are parallel with each other. Before going into details of how the control problem was solved, it is necessary to explain how the system is transformed into the coordinates used in the calculation. As mentioned in Section 3.1, the test rig is mainly made by two independent mechanical frames connected by four actuators. Figure 24 shows a sketch of the two frames with the important elements labelled. Each frame has a fixed set of axes: normal denotation for the lower frame and prime denotation for the upper frame. Therefore, the four lower frame corners are labelled as Z_i where i is one to four, depending on the corner. Meanwhile, the upper frame corners are labeled as Z'_i. The middle points are named as Z and Z' for the lower and upper frame respectively. These labels represent the heave position (z axis) of the different points. As mentioned before, the coordinate system is fixed and it does not move with the movement of the frames. Hence, the values of these Zs are relative to the coordinate system.

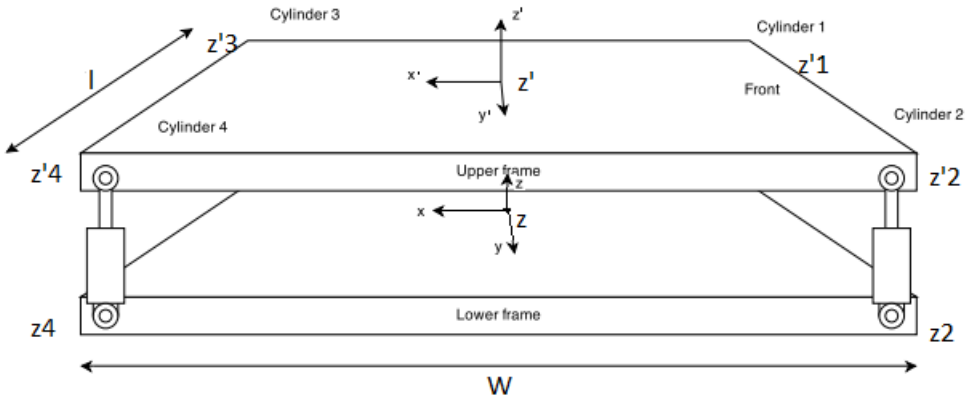

Figure 24: Frames sketch

The position of all the corners of each frame can be calculated if heave position, pitch angle and roll angle of the frame are known. These three values for the lower frame are read by the IMU. The positions of the upper frame corners are equal to the lower ones plus the actual

extension of the actuators in the different corners. The following equations show how to calculate the heave of lower frame corner by using heave (Z) of the middle point, pitch angle (θ) and roll angle (ϕ):

$$z_1 = z + \frac{w}{2} \times sin(\theta) - \frac{l}{2} \times sin(\phi) \tag{22}$$

$$z_2 = z + \frac{w}{2} \times sin(\theta) + \frac{l}{2} \times sin(\phi) \tag{23}$$

$$z_3 = z - \frac{w}{2} \times sin(\theta) + \frac{l}{2} \times sin(\phi) \tag{24}$$

$$z_4 = z - \frac{w}{2} \times sin(\theta) - \frac{l}{2} \times sin(\phi) \tag{25}$$

where w and l are the width and length of the test rig respectively in mm. Z is in mm, θ and ϕ are in rads and they are read by the IMU.

In order to simplify the calculations, small angle approximation was used. It is a simplification of basic trigonometric functions which is accurate when the angle is closed to zero. This truncation gives:

$$sin(x) = x \tag{26}$$

In the system, due to physical limitations, the maximum pitch angle is 5° and the maximum roll angle is 9.5°. The error by Equation (26) is less than 1% when the angle is smaller than 14°, so this assumption is completely valid for this system. By utilizing Equation (26), the equations Equation (22) to Equation (25) are modified into:

$$z_1 = z + \frac{w}{2} \times \theta - \frac{l}{2} \times \phi \tag{27}$$

$$z_2 = z + \frac{w}{2} \times \theta + \frac{l}{2} \times \phi \tag{28}$$

$$z_3 = z - \frac{w}{2} \times \theta + \frac{l}{2} \times \phi \tag{29}$$

$$z_4 = z - \frac{w}{2} \times \theta - \frac{l}{2} \times \phi \tag{30}$$

As a result, on the lower frame, the four heave positions of four corners can be drawn from the three middle point coordinates (heave Z, pitch θ and roll ϕ).

In the case of the upper frame, the heave positions are obtained by:

$$z_1' = z_1 + Pos_1 \tag{31}$$

$$z_2' = z_2 + Pos_2 \tag{32}$$

$$z_3' = z_3 + Pos_3 \tag{33}$$

$$z_4' = z_4 + Pos_4 \tag{34}$$

$$z' = \frac{z_1' + z_2' + z_3' + z_4'}{4} \tag{35}$$

$$\theta' = \frac{z_2' - z_3'}{w} \tag{36}$$

$$\phi' = \frac{z_2' - z_1'}{l} \tag{37}$$

where Pos_i (i=1,2,3,4) is the position of the actuator.

The decoupling of movements allows to treat each actuator independently. Therefore, each actuator is an independent system with its own controller. The reference sent to each actuator is the inverted Z_i that is calculated with Equation (27) to Equation (30). If the corner Z_i moves an increment $\Delta(Z_i)$, the reference sent to controller is $-\Delta(Z_i)$ as explained in Figure 25. The efficiency of the system in terms of vibration redaction in the upper frame is attained by a comparison between Z, θ, ϕ and Z', θ', ϕ'.

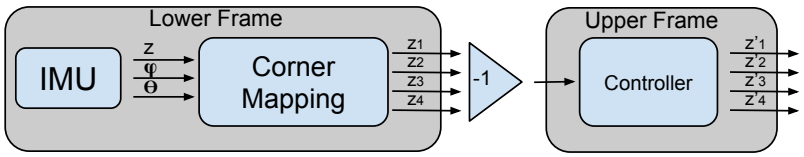

Figure 25: Control flow

4.4.2 Velocity Controller

PID The first experiment was to create a single PID controller for the velocity. However, due to the nonlinear behavior of the system, the velocity output is not always stable within different input reference ranges. The controller is working for a small reference range, close to linearization point. However, if the reference is far from the linearization point, the velocity output becomes unstable.

Gain Scheduling Controller Stable performance of the controller was desired for all input references, so it was decided to use a nonlinear approach called gain scheduling. This method was selected over the other ones studied due to its intuitiveness and robust characteristics in the presence of system nonlinearities. The author of this project had more experience in this approach, so better optimisztion and results could be achieved. This method, as explained in Section 2.4.4, consists of linearizing the nonlinear model at different operating points. After the model has been linearized several times, an unique controller is tuned for each linear model. In this application case, the model was linearized 20 times on 20 operation points, since it was the number that gave the best performance after experiments. A specific PID controller was tuned for each linear model. Figure 26 shows the controller performance and proves that the model is a good approximation of the real system, since they behave in a similar way.

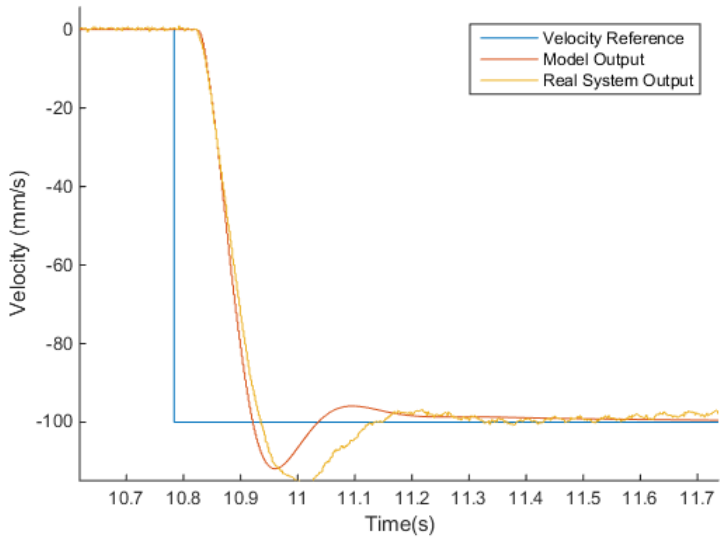

Figure 26: Velocity of the actuator output after gain scheduling for both model and real system

4.4.3 Position Controller

Cascade Controller In addition to the velocity controller, a position controller was designed in a cascade combination with the velocity controller. Figure 27 represents the controller block diagram. Therefore, the system is controlling position and velocity at the same time. Figure 28 and Figure 29 illustrate both the real system and model with the position controller behave similarly under a step and a sine wave reference signal. All the tests were carried out on one single actuator.

The step disturbance input is not a real signal that the forwarder can meet. As mentioned in Section 2.3, the maximum acceleration a forwarder can be exposed to is around 0.6-1 m/s^2. A step reference corresponds to an ∞ acceleration of the vibration. Nevertheless, this step disturbance was tested for investigating the correctness of the controller.

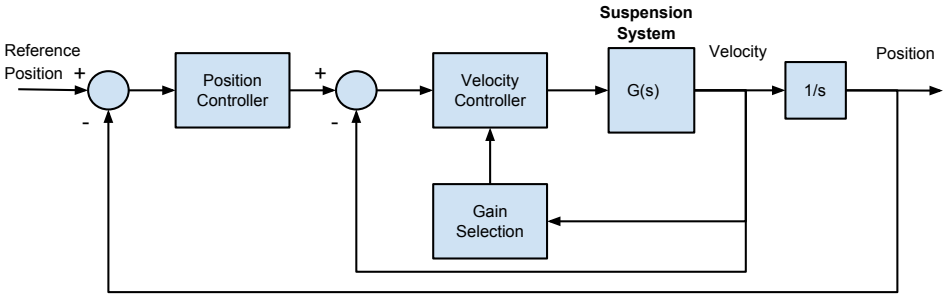

Figure 27: Position plus velocity controller block diagram.

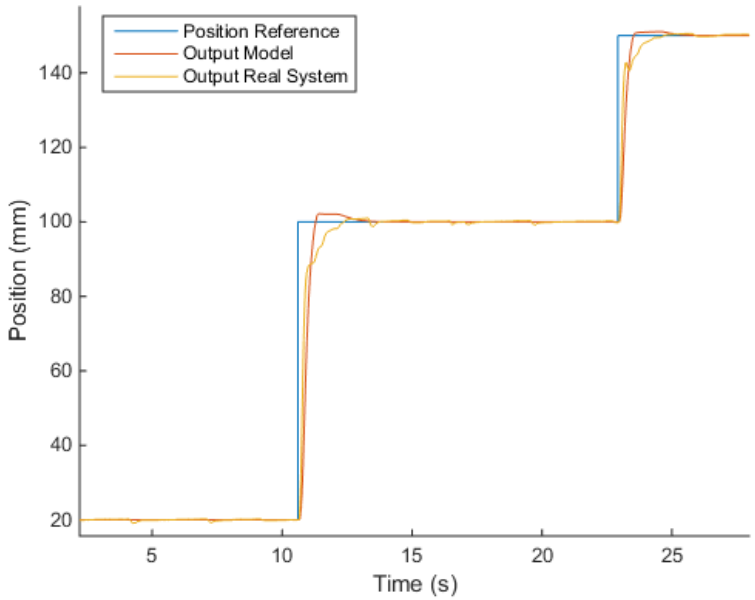

Figure 28: Position of the actuator with a step as an input

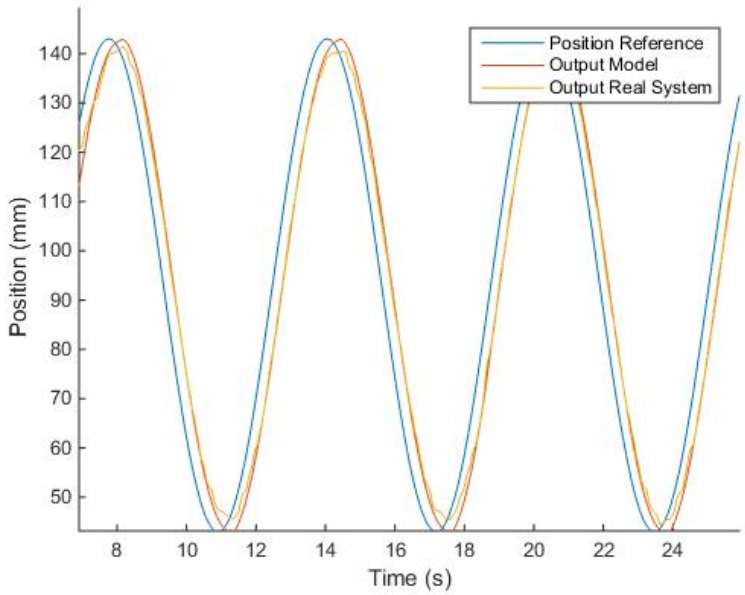

Figure 29: Position of the actuator with a sine wave as an input

4.5 Smith Predictor

The system has a delay of around 36 ms, so a control method has to be implemented to decrease the effect of the delay. Hence, Smith Predictor was implemented as described in Section 2.5. A controller performance comparison between the system with and without Smith Predictor is shown in Figure 30 which proves that the system with Smith Predictor has a faster and smoother response.

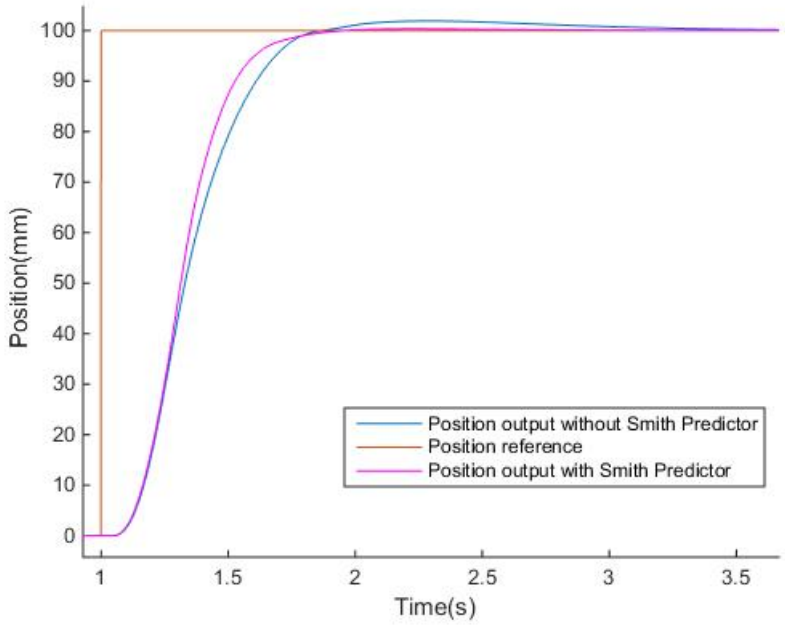

Figure 30: Comparison of controllers with and without Smith Predictor

In order to have a better overview of the control system, the Simulink model for the actuator controller has been attached to Part III. In Figure 51 is introduced the block system for one single actuator. Each actuator has a similar and independent system as the one shown. Figure 52 explains how the controller vary the gains according to the operating point the real system is. In addition, the respective gains chosen with the scheduling are sent to the controller which its Simulink block is Figure 54. Finally, Figure 53 helps to understand how the Smith Predictor is able to reduce the effect of the delay using a ideal model with no delay. This is the approach used for obtaining the result of this project.

5 Result

This chapter describes the results of the different implementations done during the project. The Equation (38) was used to calculate the percentage of vibration reduction,

$$Damp_{\%} = \frac{A_{Lower} - A_{Upper}}{A_{Lower}} 100 \tag{38}$$

where $Damp_{\%}$ is the percentage of the total vibration amplitude that is damped out, A_{Lower} is the movement amplitude of the lower frame and A_{Upper} is the movement amplitude of the upper frame.

The results explained in this section were gathered both from the model and the real system. The tests in Section 5.1 and heave test in Section 5.3 were conducted without using the IMU and Steward platform. This decision is based on the following reasons:

- Due to the fact that the valve is still a prototype, the pilot springs that move the spools are not strong enough to handle high stress. Therefore, a simple test environment was preferred to check the correctness of the controller before including all the system parts in case of valve failure.
- The IMU outputs are acceleration (x, y, z) and angular velocity (pitch and roll). As the implemented controller uses positions and angles as reference, it is necessary to integrate twice the linear acceleration and once the angular velocities. In order to have a precise position reference, high pass filters need to be designed to avoid the drift of the signal due to errors in the integration. This leads to phase shifting, which is extremely difficult and time consuming to synchronize and calibrate the position and angles signal derived from the IMU readings.

Therefore, in the tests in Section 5.1 and heave test in Section 5.3, the movement of the lower frame was simulated and the frame that was actually moving was the upper frame. This means that the reference sent to the controller was obtained from simulation and the control output was sent to the valves which controlled the movement of actuators. During the realization of the heave test in Section 5.3, two valves broke. They were sent to be repaired but the replacements did not come on time. Hence, the IMU and Steward platform could not be used. Since the model has been proved to behave almost same as the real system, the rest of the tests are model based.

5.1 Performance of Suspension System in the Test Rig

Figure 31, Figure 32 and Figure 33 illustrate the vibration reduction performance in the real system with vibrations of heave, pitch and roll respectively. The controller used was the normal gain scheduling controller for the velocity plus the position controller in cascade. The input vibration had an amplitude of 60 mm for heave, 3.5° (0.06 rads) for pitch and 8.8° (0.14 rads) for roll at 0.5 Hz.

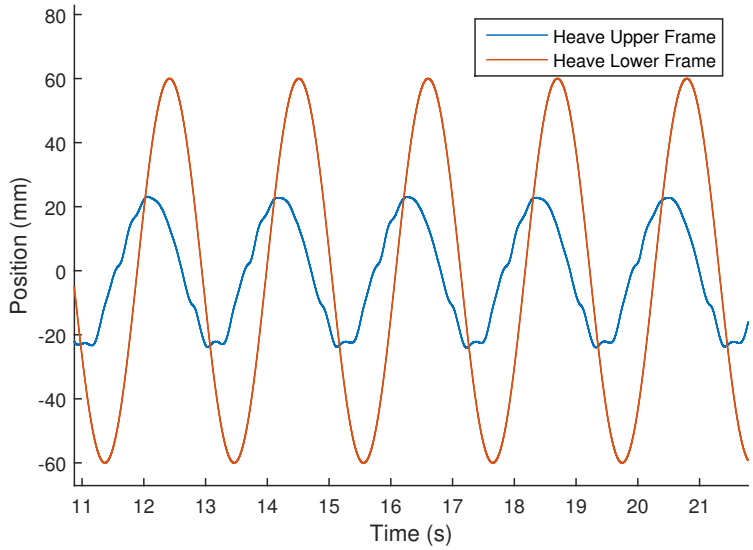

Figure 31: Heave of lower and upper frame in the real system.

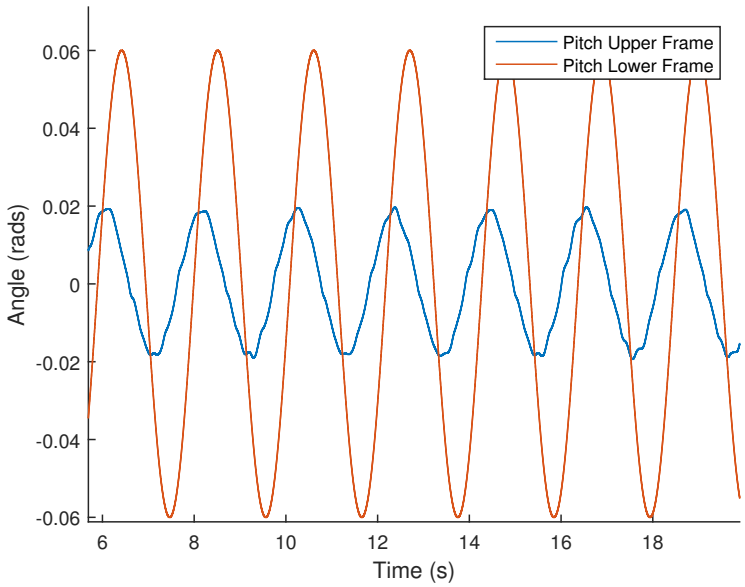

Figure 32: Pitch of lower and upper frame in the real system.

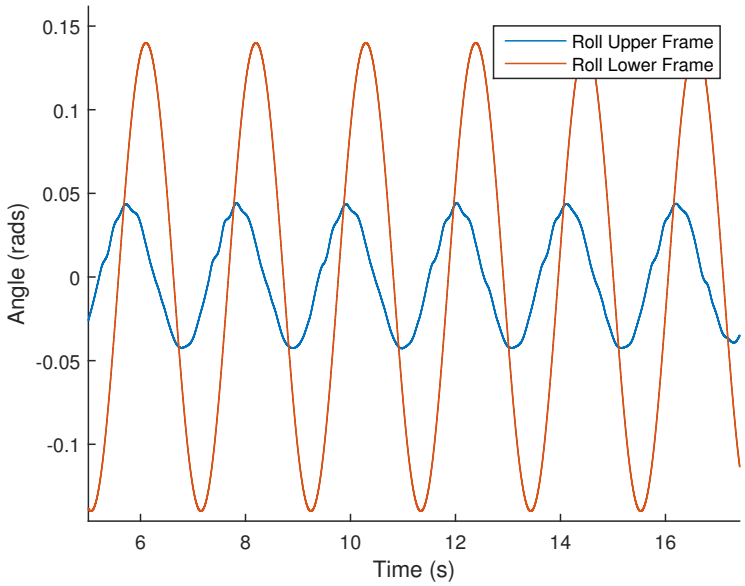

Figure 33: Roll of lower and upper frame in the real system.

From the pictures above, it can be calculated that the total percentages of the vibration damped are $Damp_{\%} = 63\%$ for heave, $Damp_{\%} = 66.67\%$ for pitch and $Damp_{\%} = 68\%$ for roll.

5.2 Comparison System with and without Delay

The delay reduction is one of the main concerns since the beginning of the project. Therefore, a comparison between the system with delay and the system without delay (ideal system) needs to be performed in order to gain an idea of how much the delay affects the system performance. For doing so, a new model without the delay was estimated. A model based test was set for comparing both models with and without delay. The input vibration had an amplitude of 60 mm for heave, 3.5° (0.06 rads) for pitch and 8.8° (0.14 rads) for roll at 0.5 Hz. Figure 34, Figure 35 and Figure 36 contain the comparison results for heave, pitch and roll respectively.

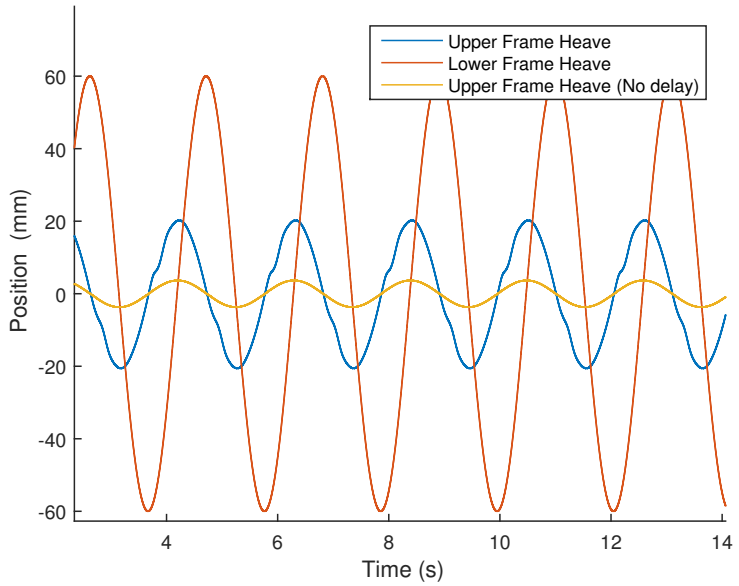

Figure 34: Heave comparison delay vs. no delay.

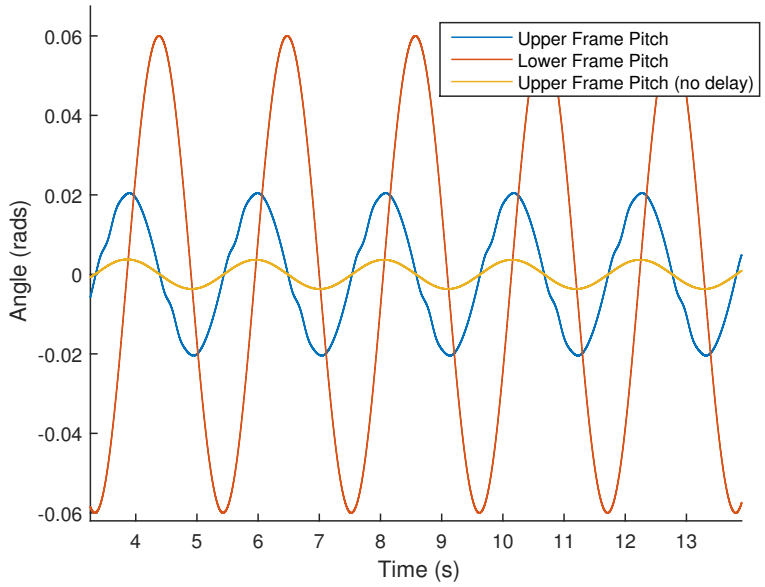

Figure 35: Pitch comparison delay vs. no delay.

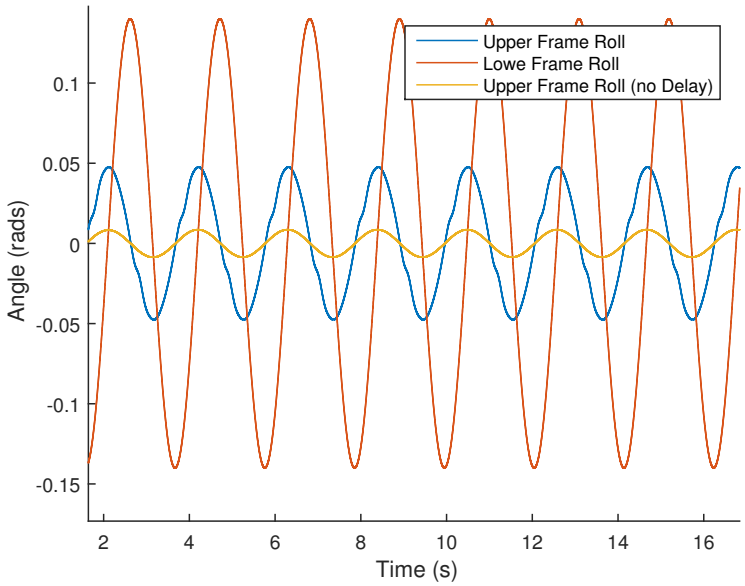

Figure 36: Roll comparison delay vs. no delay.

For the real system with delay, the percentages of the vibration reduction are $Damp_{\%} = 66.67\%$ for heave, $Damp_{\%} = 66.67\%$ for pitch and $Damp_{\%} = 68\%$ for roll. In conclusion, the model simulation results and real system results obtained in Section 5.1 are very close. Therefore, it is deemed that the model is a good estimation of the real system.

The percentages of the vibration reduction in the system without delay or ideal system are $Damp_{\%} = 93.9\%$ for heave, $Damp_{\%} = 93.67\%$ for pitch and $Damp_{\%} = 94\%$ for roll.

5.3 Performance of Smith Predictor

Since the reduction of the delay really affects the performance of the suspension system, a Smith Predictor controller mixed with gain scheduling was designed to decrease the effect of the delay. This new approach was compared with the controller tested in the previous sections. The test case was conducted in the real system with a heave vibration amplitude of 60 mm and 0.5 Hz frequency. Figure 37 shows how this new method outperforms the normal gain scheduling controller. Right after testing the heave with the Smith Predictor controller, the spring in one of the valves broke. The vibration reduction of the system with Smith Predictor is $Damp_{\%} = 77.5\%$ for heave.

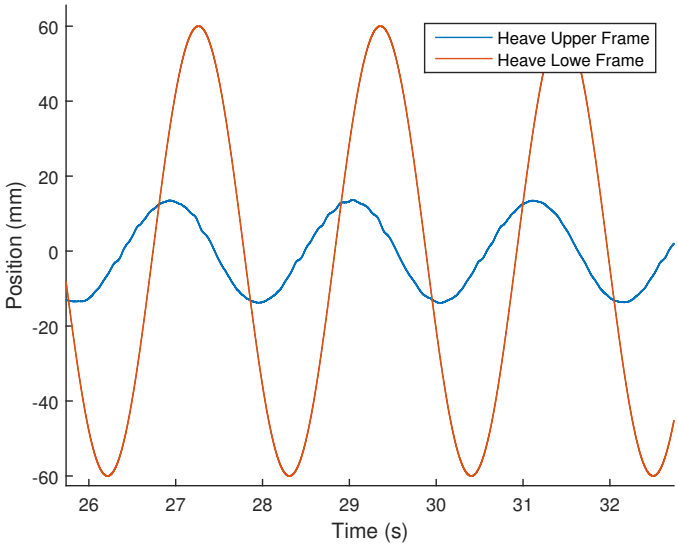

Figure 37: Heave in the real system using Smith Predictor.

In order to verify that Smith Predictor has a better performance, the same tests were done in the model with both Smith Predictor controller and normal gain scheduling controller. The results are plotted for heave in Figure 38, pitch in Figure 39 and roll in Figure 40.

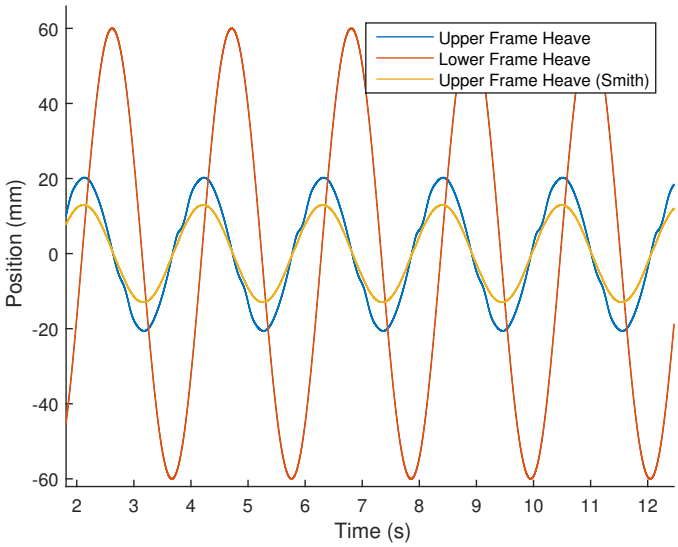

Figure 38: Heave comparison delay vs. Smith Predictor

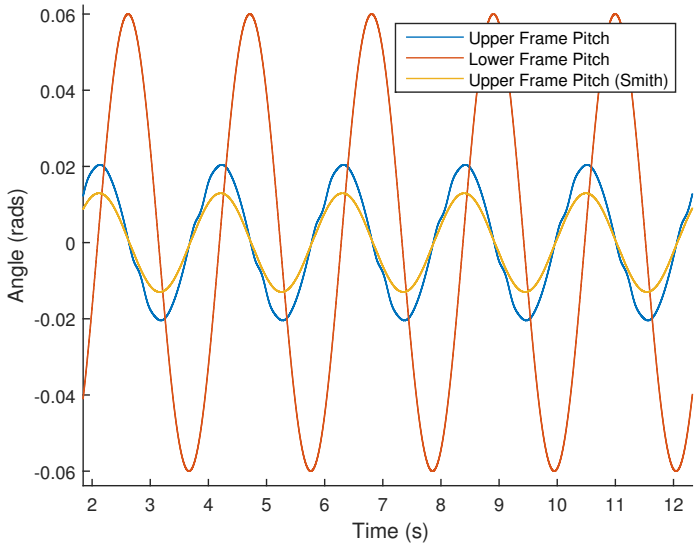

Figure 39: Pitch comparison delay vs. Smith Predictor

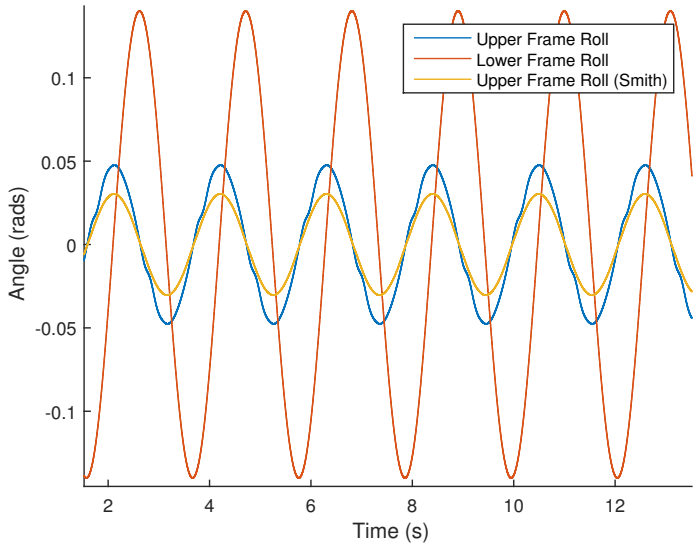

Figure 40: Roll comparison delay vs. Smith Predictor

The vibration reduction performances of the model with Smith Predictor are $Damp_{\%} = 78.45\%$ for heave, $Damp_{\%} = 78.41\%$ for pitch and $Damp_{\%} = 78.57\%$ for roll. As discussed in Section 5.1, it has been proven that the Smith Predictor controller can reduce the vibration around 12% more than the normal gain scheduling controller for all three movements.

5.4 Result of Test Cases

In this section, different test cases with different vibration amplitudes and frequencies are presented. The description of the vibration has the amplitude for heave, pitch and roll, the vibration frequency, the maximum acceleration of the actuators and the maximum flow needed for the hydraulic system. In Table 1, heave, pitch and roll are tested individually. In Table 2, a combination of these three motions are combined for creating a complex vibration. In both tables, $\times$ means that the controller is amplifying the vibration instead of damping it, and Kp is the gain of the position controller. $Mode1$ is the control system with delay, $Mode2$ is the control system without delay or ideal system and $Mode3$ is the control system with delay but using Smith Predictor controller.

Table 1: Test of heave, pitch and roll (independently) for different amplitudes and frequencies

Test case	Description						Mode1 efficiency (%)	Mode2 efficiency (%)	Mode3 efficiency (%)
	Heave amp. (mm)	Pitch amp. (degree)	Roll amp. (degree)	F (Hz)	Max acc. (mm/s^2)	Max flow (l/min)			
1	20	0	0	0.5	180	18.2	66.7	94.0	83.2
2	60	0	0	0.5	630	54.5	66.7	94.0	83.0
3	20	0	0	1	720	36.2	33.0	76.0	66.0
4	60	0	0	1	2160	108.5	27.0	76.0	65.3
5	20	0	0	1.5	1620	54.4	3.7	65.0	45.7
6	40	0	0	1.5	3239	108.4	$\times$	65.0	$\times$(Kp=18) 25(Kp=13)
7	20	0	0	2	2880	73.3	$\times$	54.8	21.6
8	10	0	0	2	1440	36.2	$\times$	55.3	28.2
9	0	4	0	0.5	583	48.1	66.1	87.9	83.1
10	0	3.4	0	1	1998	80.0	6.4	75.6	65.1
11	0	1.7	0	1.5	2248	60.1	$\times$	65.1	45.7
12	0	1.2	0	2	2664	56.5	$\times$	55.2	23.5
13	0	0	9.2	0.5	742	60.1	66.2	87.9	83.3
14	0	0	6.3	1	2039	82.5	29.5	75.9	64.9
15	0	0	4.0	1	1300	52.3	32.8	76.0	65.0
16	0	0	2.9	1.5	2085	57.0	0	65.0	45.6
17	0	0	2.3	1.5	1668	45.2	3.3	65	45.5
18	0	0	1.7	2	2225	44.7	$\times$	55	26.7
19	0	0	1.2	2	1483	31.4	$\times$	55	27.5

Table 2: Test of combination of heave, pitch and roll for different amplitudes and frequencies

Test case	Description						Mode1 efficiency (%) Heave Pitch Roll	Mode2 efficiency (%) Heave Pitch Roll	Mode3 efficiency (%) Heave Pitch Roll
	Heave amp. (mm)	Pitch amp. (degree)	Roll amp. (degree)	F (Hz)	Max acc. (mm/s^2)	Max flow (l/min)			
1B	20	2.3	1.7	0.5	652	30.6	66.5 66.5 66.5	92.5 92.5 92.5	83.1 83.1 83.1
2B	38	1.7	2.9	0.5	823	40.0	66.6 66.6 66.6	94.0 94.0 94.0	83.1 83.1 83.1
3B	20	2.3	1.7	1	2608	61.8	35.7 1.0 ×	87.8 6.25 ×	64.8 51.1 25.5
4B	10	0.6	1.2	1.5	2394	40.1	6.0 × ×	81.8 84.2 82.0	45.0 40.1 44.0
5B	5	0.6	0.6	1.5	1571	24.9	6.0 4.0 0.1	82.0 82.0 82.0	44.0 46.0 45.7
6B	5	0.6	0.6	2	2794	32.8	× × ×	76.0 × ×	26.8 21.5 16.5
7B	5	0.6	0.6	2	2030	31.0	× × ×	76.7 76.3 76.2	20.0 21.0 18.0

The results shown in the tables are explained in Section 6.

5.5 Real Track Test

Skogforsk has a test track formed by different bumps. It simulates all the possibilities in a forest in terms of ground irregularities. A 3D model of the track is represented in Figure 41 and more detailed information is depicted in Figure 42.

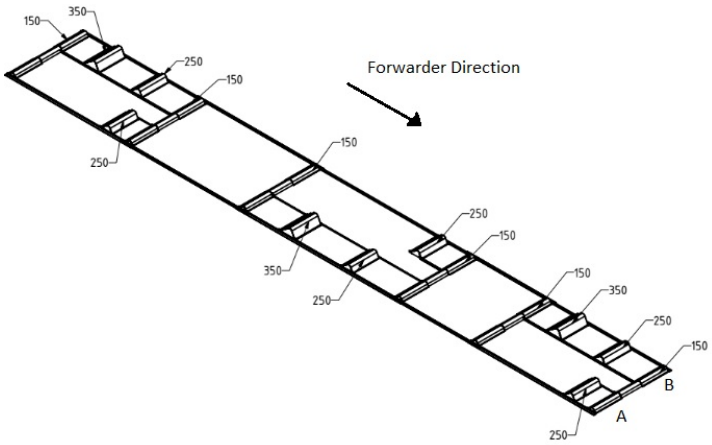

Figure 41: 3D track model

The track has two different halves, A and B which are labeled in Figure 41. Each half is for one set of the machine wheels. The track has a fixed length and the forwarder needs to keep a constant velocity during the test. The total length of the track is 57 m which must be crossed in 90 s. This requirement sets the forwarder velocity to be 30 m/min during the test.

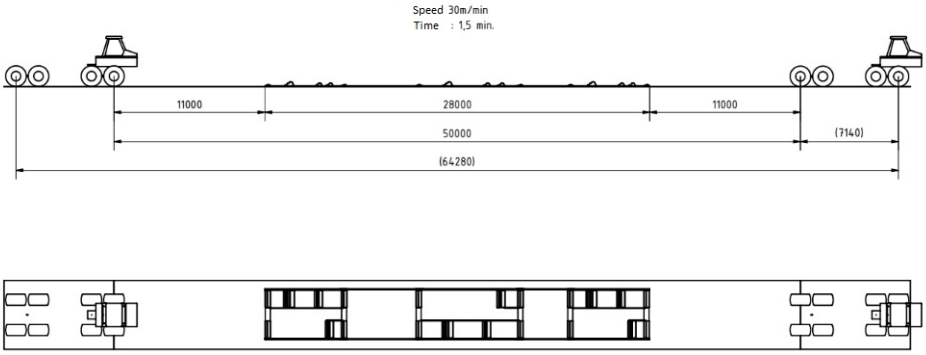

Figure 42: CAD track model

Besides the active cab suspension designed in this project, there is another suspension mechanism in the forwarder which aims to absorb vibration from the rough terrain to the main frame. This mechanism could be soft tires or/and some freedom for the wheels to move. However, this system cannot reduce the vibration in the main frame completely. Therefore, vibration reductions are supposed to be 60% for heave, 40% for pitch and 30% for roll, then the vibrations left for the main frame are 40% for heave, 60% for pitch and 70% for roll. Furthermore, since this mechanism was not the main concern of this project, it was not studied in depth.

The simulation done in this project only considered the front wagon that is composed of four wheels. The dimensions of it were obtained from the Part III. Hence, after knowing the dimensions of the machine, the track profile and the speed of the forwarder, the wheels vertical

displacement over time can be calculated. Figure 43 and Figure 44 show the vertical positions of the left and right front wheels respectively. The positions for the rear wheels are the same but time shifted because they meet the bumps after the front wheels.

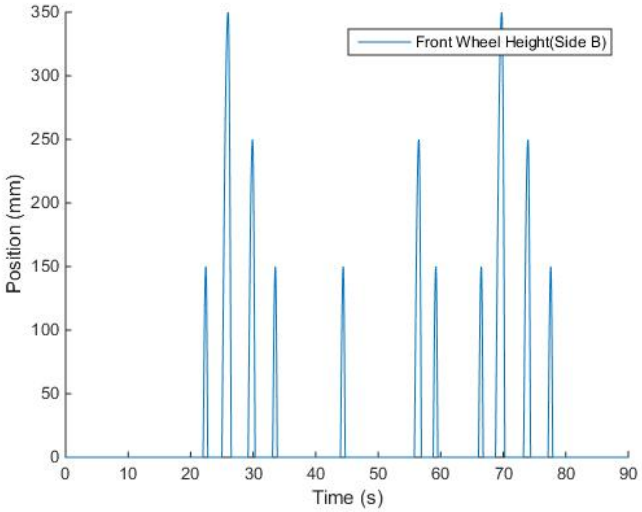

Figure 43: Left wheel

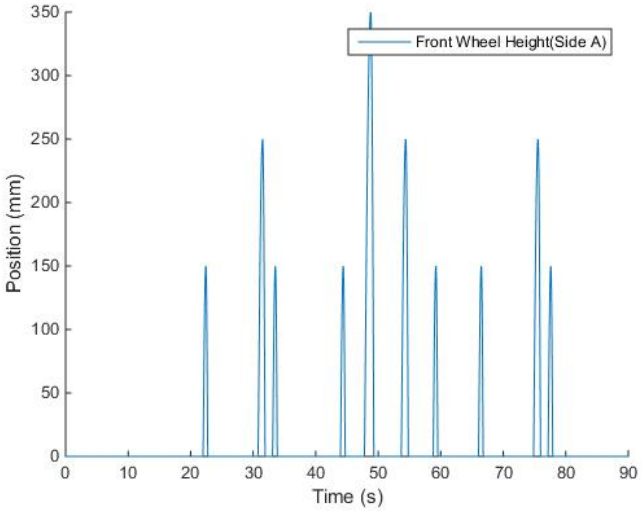

Figure 44: Right wheel

With the help of the equations introduced in Section 4.4.1 and applying the damping efficiency previously mentioned for the wheels suspensions, the heave displacement, pitch and roll angles of the lower frame are obtained. Figure 45, Figure 46 and Figure 47 show the absolute displacements of the lower and upper frame for heave, pitch and roll respectively with the different control approaches. The figures are zoomed to a small time region in order to have a better understanding and to clearly see the results. The results are discussed in Section 6.

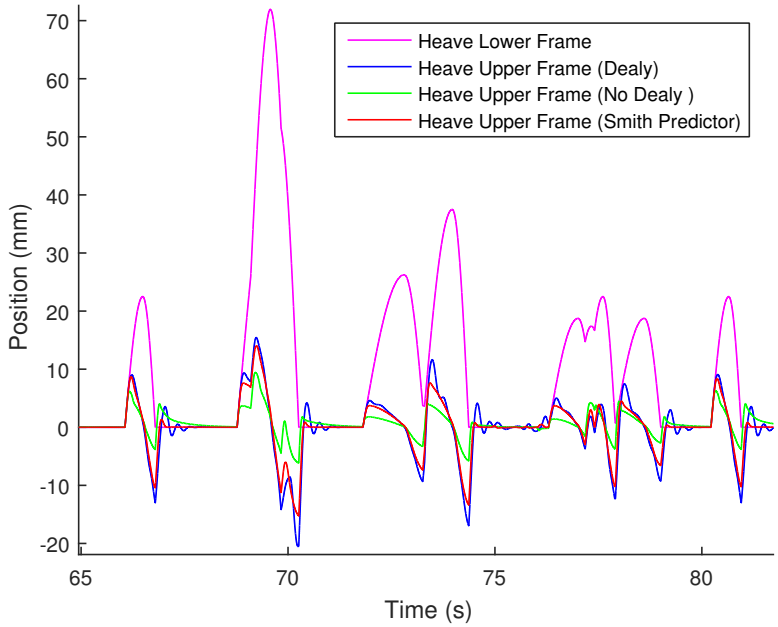

Figure 45: Heave displacement of the lower and upper frame using the test track data

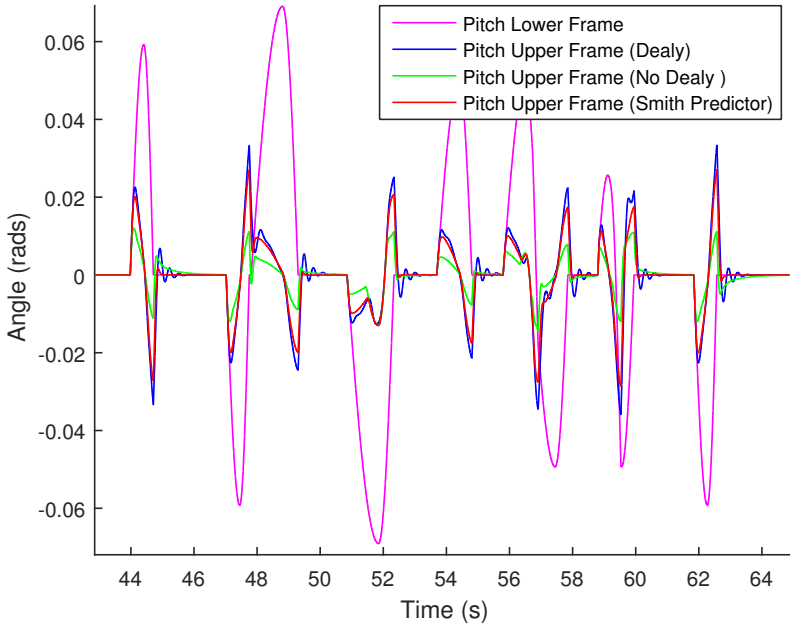

Figure 46: Pitch displacement of the lower and upper frame using the test track data

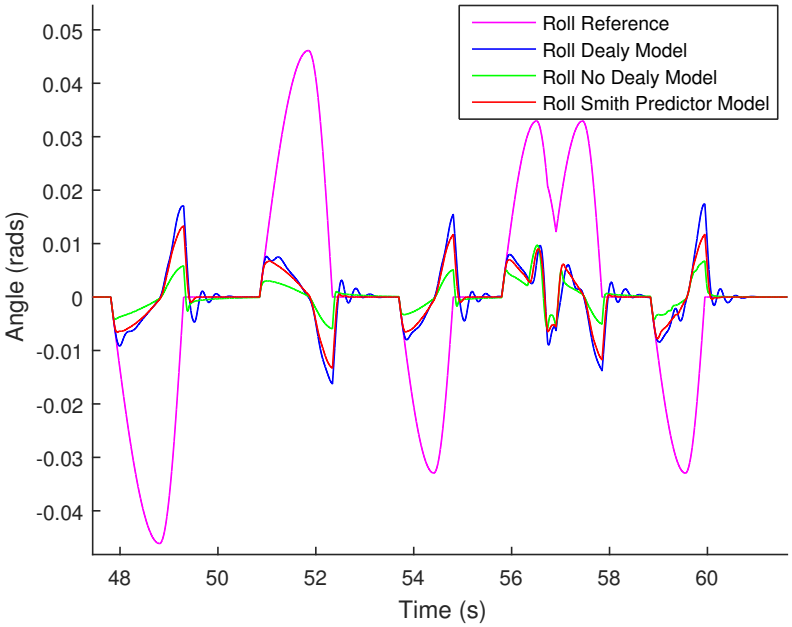

Figure 47: Roll displacement of the lower and upper frame using the test track data

5.6 Efficiency and Energy Consumption

The power consumed by an actuator can be calculated with the following equation:

$$P_c = p_{in} Q_{in} \tag{39}$$

where P_c is the power consumption in watt, P_{in} is the meter-in pressure in pascal and Q_{in} is the meter-in flow in m^3/s.

In Figure 48, the pressure of both A and B ports as well as the velocity of one actuator are presented. The data plotted was recorded in the test as presented in Section 5.1. The maximum consuming power is reached when the actuators are extending with the load. When the actuators are extending, the meter-in pressure is in the A port. The meter-in flow was calculated by multiplying the actuator velocity by the piston side area. The value of the velocity used for the calculation was the peak value or maximum velocity.

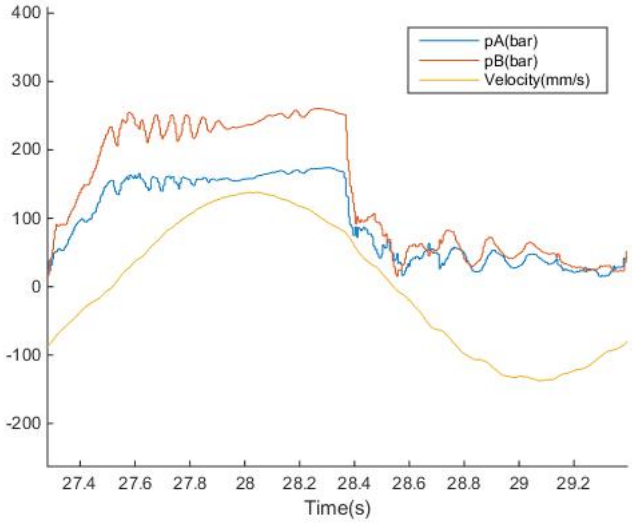

Figure 48: Pressure for port A and B and the velocity of one actuator

The total power computation of the suspension system was obtained by summing the individual power consumption of each actuator. The final power consumed by the system is 11.63 kW. This value is the maximum instant power consumed by the system but not the average.

6 Discussion and Conclusion

The first set of test cases in Section 5.1 was conducted on the real test rig. For the realization of these tests, the lower frame was simulated as explained in Section 5. A defect in the pilot spring of the valve was reminded and warned by the valve provider. The valves used in this project are still a prototype version. Since the spring could break at any moment, it was decided to gather the results without incrementing the complexity of the system with the IMU and Stewart platform at first. Therefore, a vibration reference was created in Simulink in order to mimic how the lower frame moved. The reference was mapped, inverted and sent to the four real actuators which moved the upper frame. Finally, the absolute movement of the upper frame was compared with the absolute movement of the lower frame.

The spool opening range used for the real test rig was from -2 to 2 mm. Although the maximum spool opening is 3.5 mm for both positive and negative directions, it was not desired to push the test rig to the limit in the first set of tests in case of valve malfunctioning. The first controller tested in the real system was a normal gain scheduling PID controller for the velocity plus a position controller in a cascade structure as shown in Figure 27. Heave, pitch and roll were tested individually. The frequency of the vibration used for the test was 0.5 Hz. The heave amplitude was 60 mm, the pitch amplitude was 3.5° and 8.8° for roll amplitude. It can be seen that the total disturbance reductions are 63% for heave, 66.67% for pitch and 68% for roll.

The system delay was a concern since the beginning of the project. Hence, it was interesting to know how this delay affected the performance of the system. Therefore, a new set of model based tests was performed. In these new tests, an ideal model or model without delay was estimated and compared with the model of the actual system. In this way, the effects of the delay can be identified clearly. The disturbance used in this test set had a 0.5 Hz frequency and a heave amplitude of 60 mm, a pitch amplitude of 3.5° and a roll amplitude 8.8°. From Section 5.2, the following results are extracted:

- System with delay: the total disturbance reduction percentages are 66.67% for heave, 66.67% for pitch and 68% for roll.
- System without delay or ideal system: the total disturbance reduction percentages are 93.9% for heave, 93.67% for pitch and 94% for roll.

The results prove that reducing the delay increases drastically the efficiency of the system in terms of vibration reduction. Moreover, compared with the results obtained from the real system, it illustrates that the model is very closed to the real system, since the results are almost the same in both cases.

In order to reduce the effect of the delay, a new control method was applied. The chosen method was Smith Predictor, since it is intuitive but still effective. A comparison between the controller with and without Smith Predictor was discussed in Figure 30 where Smith Predictor controller acted faster and with less overshoot than the normal gain scheduling controller. Smith Predictor controller was tested in the real system with the same vibration signal used in the

previous tests. Nevertheless, when the heave was being tested, one of the valves broke. As a result, it was impossible to continue testing the controller on the real rig. Fortunately, the heave data was recorded. The vibration signal had 0.5 Hz frequency and a heave amplitude of 60 mm. The percentage damped out of the total vibration with Smith Predictor controller is 77.5% which is 15% higher than the normal gain scheduling controller.

Without the possibility of continuing using the rig, it was decided to continue the left tests by using simulation. Furthermore, since the model used is a very good approximation of the real system, the results should be close to the ones that would have been obtained from the real system. In Section 5.3, a comparison between normal gain scheduling controller and Smith Predictor controller was conducted. The vibration used had a 0.5 Hz frequency and a heave amplitude of 60 mm, a pitch amplitude of 3.5° and a roll amplitude of 8.8°. From the results:

- System with normal gain scheduling controller: the total disturbance reduction percentages are 66.67% for heave, 66.67% for pitch and 68% for roll.
- System with Smith Predictor controller: the total disturbance reduction percentages are 78.45% for heave, 78.41% for pitch and 78.57% for roll.

It can be concluded that the Smith Predictor improves the performance of the active suspension for all three movements.

More test cases were done in the real test rig with different amplitudes and frequencies of the vibration. However, due to the lack of spare valves, it was decided to create different test cases with different configurations in the simulation. For the simulation test cases, the spool position range was from -2.4 to 2.5 mm. The spool position was not increased more, since the actuators reached almost 1 m/s which is the maximum speed they can handle due to mechanical limitations. Moreover, in all of these test cases, the maximum vibration frequency is 2 Hz, since for higher frequency, the performance of the controller starts decreasing and the actuators need to reach accelerations above 3 m/s^2 which is far from the vibration acceleration a forwarder would meet. The results have been summarized in Table 1 and Table 2. The conclusions drawn from Table 1 are:

- For a disturbance with the same amplitude, if the frequency increases, the damping efficiencies decreases for all of three modes. Then, the faster the system responds, the better the damping efficiency is. Hence the best control performance is observed in the system without delay or ideal system and the worst is the normal gain scheduling controller without Smith Predictor. For example, in test case 7, the normal gain scheduling controller amplifies instead of damping the vibration in the upper frame. Meanwhile the ideal system reduces the vibration of 54.8% and the Smith Predictor controller reduces it of 21.6%.
- When the acceleration peaks in the vibrations do not go above 2.5 m/s^2, the controller works correctly. A vibration has a high acceleration value when both its amplitude and frequency are high. As a result, the control performance decreases for high acceleration. As mentioned in Section 2.3, the acceleration of vibrations for a forwarder is usually no

more than 1 m/s^2. Thus the controller can handle the operating vibrations well under the acceleration of 1 m/s^2.

- When the vibration changes too fast, the controller amplifies the vibration as shown in test case 6. In this test case, the Smith Predictor controller uses a position controller gain of 18 which results in amplification of the vibration. However, if the gain is reduced to 13, the controller becomes less aggressive and is able to reduce the vibration of 25%.
- The maximum flow consumption during the operation of the suspension system is 108.4 l/min. The suspension system is the main hydraulic system consuming flow when the forwarder is moving. Therefore, this maximum value of flow is not considered as too high. Moreover, this flow is the peak value and it is not maintained during the whole operating time. Meanwhile, hydraulic accumulators could be used for reaching peak flow values.

In Table 2, heave, pitch and roll are combined at the same time for creating different complex vibrations. There are some conclusions drawn from Table 2 as well. If all the motions have the same phase, it is an extreme case for the suspension system. This is because if they have the same phase, it results in higher amplitude movements for some cylinders. On the contrary, if they have offsets between each other, part of the vibrations are cancelled between each other, which provides less work to the suspension system. In order to demonstrate this phenomenon, two test cases 6B and 7B were conducted. The difference between these two tests is a phase change in test case 7B. As a result, the controllers in test case 7B produces a higher damping efficiency than in test case 6B.

The real track test reveals interesting results. The duration of the test is 70 s in total. However, it was zoomed into interesting time range, making it more understandable and visible. Section 5.5 shows the following results:

- System with normal gain scheduling controller: the total disturbance reduction percentages are 70% for heave, 63% for pitch and 68% for roll.
- System with Smith Predictor controller: the total disturbance reduction percentages are 75% for heave, 68% for pitch and 73% for roll.
- System without delay or ideal system: the total disturbance reduction percentages are 85% for heave, 83% for pitch and 90% for roll.

In conclusion, the Smith Predictor controller has a smoother response with less overshoot and oscillation than the normal gain scheduling controller. When the vibrations change fast and with small amplitude, the system takes time to react. Therefore, it is believed that a passive suspension element can cope with this small amplitude and high frequency vibration.

Regarding the efficiency, it has been chosen a small forwarder engine of 127 kW as a reference. The maximum amount of power needed during the forwarder operation is 11.63 kW which is around 15 horsepower. Consequently, the amount of power needed is around 10% of the maximum power provided by the engine. Moreover, 11.63 kW is the momentary maximum

power, so the average power is less during the whole application. It can be concluded that this amount of power is not significant and this system is affordable to be incorporated in a forwarder. Nevertheless, during the realization of this test, there was no cab on top of the test rig. Introducing a cab in the system means increasing the load weight and, therefore, more power is needed for moving the extra weight so further study has to be done in the future.

One interesting phenomenon observed in Figure 28 is that there is a slow behavior when the real system is reaching the position reference. The reason for this phenomenon is that there is a slow pole in the closed loop transfer function that is governing the response of the system. This slow pole is due to dynamics that is not included in the model of the real system. It is deemed that this dynamics is the fluid dynamics. The controller was created with a second order model and not taking into account the fluid dynamics, so this slow pole cannot be influenced with the actual controller. That is the reason why no mater how the parameters of the controller are tuned, it is not possible to get rid of this slow behaviour. Therefore, in order to influence the slow pole, a higher order model is necessary. To do this, the pressure as well as the force have to be controlled. This could have been done if the theoretical model were working. Nevertheless, the understanding of this phenomenon is not easy and further analysis needs to be continued.

7 Future Work

The designed controllers had shown good results for all types of individual movement and for combination of these movements. However, due to the problem with the broken valves, most of the test cases were done in simulation. Therefore, the first step that should be done to continue this work is to replace the broken valves and do further tests with the test rig. The test system can be modified in order to make it as close as possible to the real forwarder system. Right now, there is no cab on top of the upper frame, leading to less load on the actuators when operating the system. The cab, depending on the height and weight, creates different reactions that could affect the final behavior of the controller. Hence, a load simulating the cab, or even better, a test cab similar to the one used in the real forwarder could be attached to the upper frame. Moreover, when the controller is robust in the test application, it should be implemented in a real forwarder suspension system. A test forwarder could be used in the test track (Figure 41) in order to have almost the real conditions that a forwarder could have in the forest.

It is extremely important to calibrate the valves well. During the realization of this project, 4 valves broke in total. Every time a new valve is included, individual calibration has to be done, since it is impossible to manufacture the valves exactly the same. There are some parameters, such as the minimum current that needs to be applied to the voice coil or the spool position offset, that are crucial for the correct functioning of the valve. Therefore, wrong parameter values could cause different behaviors for both positive and negative spool movements as well as slower spool response.

Each valve has its own configuration file with more than one hundred parameters that can be changed. For the realization of this project, many parameter were tuned, such as the PID gain for the spool position controller, in order to try to improve the behaviour of the system. However, it was not possible to look through them all due to the lack of time for truly understanding the effects of the whole parameters. It is believed that better understanding of the valve is necessary in order to change the parameters in a manner that improves the behavior of the valve. Therefore, more work on this area is encouraged in order to optimize the valves to the maximum level.

Furthermore, the lack of knowledge about the valve is not only a problem for tuning the valve parameters, but also for creating a proper theoretical model of the valve. The specific opening area depending on the spool position is a critical factor that has to be tuned each time a reference is changed as shown in Section 4.3.1. Due to this factor and other nonlinearities, it was not possible to obtain a good model. If the theoretical model was working, a force controller could have been done together with a position and a velocity controller. An example is represented in Figure 4. Thus, it is necessary to do further study in order to have a theoretical model.

Other aspects that could be considered for the following project is to use pole placement for each PID controller created for each linearized plant. In this project, a PID tune function in MATLAB was used, since it was easy to change the configuration of this function to change the controller instead of conducting pole placement 20 times.

Regarding the actual valve response delay, it can be reduced to around 4 ms by installing

the actual controller algorithm directly in the valve embedded system. Therefore, it could send control signal each 4 ms, which improves the performance of the system. In order to be able to install this controller inside the valve, the controller has to be robust and revised by the valve manufacturer in order to testify if it works under the constraints of the valves.

In terms of the actual hardware that was used, the limiting factor was the valve, which is not made for this control application. A revision of the components has to be achieved in order to handle the continuous spool movement due to the control actions. The main application of this valve is in cranes for moving big load, where it is not necessary to change the spool position constantly. For the active suspension, the spool is constantly moving from positive to negative direction in order to provide the desired velocity and position of the actuator. The manufactured spring is too weak for this application, causing several failures after being used for a while. Nevertheless, even though the valves are not made for this application, they have shown good results. Moreover, these valves are cheaper than the ones used to reach high precision control and fast response.

References

[1] A. D. Herrero, "Maquinaria forestal komatsu valmet." `http://almadeherrero.blogspot.se/2012/05/maquinaria-forestal-komatsu-valmet.html`. Accessed January 25, 2016.

[2] G. Tora, *The active suspension of a cab in a heavy machine*. INTECH Open Access Publisher, 2012.

[3] Canadian Centre for Occupational Health and Safety, "Vibration-health effects." `https://www.ccohs.ca/oshanswers/phys_agents/vibration/vibration_effects.html`. Accessed January 25, 2016.

[4] B. Uzunoglu, "Active damping of a forwarder cabin," Master's thesis, Kungliga Tekniska Högskolan, 2016.

[5] dSPACE, "Compact and robust prototyping system for in-vehicle applications." `https://www.dspace.com/en/pub/home/products/hw/micautob.cfm`. Accessed January 28, 2016.

[6] S. Lajqi and S. Pehan, "Designs and optimizations of active and semi-active non-linear suspension systems for a terrain vehicle," *Strojniški vestnik-Journal of Mechanical Engineering*, vol. 58, no. 12, pp. 732–743, 2012.

[7] G. Verros, S. Natsiavas, and C. Papadimitriou, "Design optimization of quarter-car models with passive and semi-active suspensions under random road excitation," *Journal of Vibration and Control*, vol. 11, no. 5, pp. 581–606, 2005.

[8] T. Rao, R. Mohan, G. V. Rao, K. S. Rao, and A. Purushottam, "Analysis of passive and semi active controlled suspension systems for ride comfort in an omnibus passing over a speed bump," *International Journal of Research and Reviews in Applied Sciences*, vol. 5, no. 1, pp. 7–17, 2010.

[9] H. W. Paschold and A. G. Mayton, "Whole-body vibration: Building awareness in sh&e," *American Society of Safety Engineers*, vol. 56, no. 04, pp. 30–35, 2011.

[10] G. Tora, "Synthesis of the active cab suspension mechanism," *Key Engineering Materials*, vol. 542, pp. 219–231, 2013.

[11] Directorate-General for Employment, Social Affairs and Equal Opportunities, *Non binding guide to good practice for implementing Directive 2002/44/EC (Vibrations at Work)*. European Commission, 2007.

[12] M. V. Sivaselvan, A. M. Reinhorn, X. Shao, and S. Weinreber, "Dynamic force control with hydraulic actuators using added compliance and displacement compensation," *Earthquake Engineering & Structural Dynamics*, vol. 37, no. 15, pp. 1785–1800, 2008.

[13] H. K. Khalil, "Nonlinear systems, third edition," ch. 14, pp. 552–575, Prentice Hall, 2002.

[14] L. Xiao and Y. Zhu, "Sliding-mode output feedback control for active suspension with nonlinear actuator dynamics," *Journal of Vibration and Control*, vol. 21, no. 14, pp. 2721–2738, 2015.

[15] D. Karnopp, M. J. Croby, and R. A. Harwood, "Vibration control using semi-active force generators," *Engineering for Industry*, vol. 96, no. 2, pp. 619–626, 1974.

[16] Y. Hurmuzlu and O. D. Nwokah, "The mechanical systems design handbook: modeling, measurement, and control," ch. 12, pp. 207–226, CRC Press, 2001.

[17] M. Priyandoko, G.and Mailah and H. Jamaluddin, "Vehicle active suspension system using skyhook adaptive neuroactive force control," *Mechanical Systems and Signal Processing*, vol. 23, pp. 855–868, 2009.

[18] C. C. Lee, "Fuzzy logic in control systems: Fuzzy logic controller-part i," *Transportation on Systems, Man, and Cybernetics*, vol. 20, no. 2, pp. 404–418, 1990.

[19] S. Liu, Z. Huang, and Y. Chen, "Automobile active suspension system with fuzzy control," *Central South University of Technology*, vol. 11, no. 2, pp. 206–209, 2004.

[20] D. J. Leith and W. E. Leithead, "Survey of gain-scheduling analysis and design," *International journal of control*, vol. 73, no. 11, pp. 1001–1025, 2000.

[21] W. J. Rugh and J. S. Shamma, "Research on gain scheduling," *Automatica*, vol. 36, no. 10, pp. 1401–1425, 2000.

[22] F. D. Bianchi, H. D. Battista, and R. J. Mantz, *Wind turbine control systems: principles, modelling and gain scheduling design.* Springer Science & Business Media, 2006.

[23] MathWorks, "Plant Models for Gain-Scheduled Control." `http://www.mathworks.com/help/control/ug/plant-models-for-gain-scheduled-control.html`, 2016. Accessed April, 2016.

[24] E. F. Camacho and C. B. Alba, "Model predictive control," pp. 13–27, Springer Science & Business Media, 2013.

[25] T. Glad and L. Ljung, "Control theory," p. 383, CRC press, 2000.

[26] Q. Zhong, "Robust control of time-delay systems," ch. 2, pp. 17–43, Springer, 2006.

[27] Great Lakes TPA, "Rig frames 3d model." `http://gltpa.org/magazine/2015/november/prod-showcase.html`. Accessed January 28, 2016.

[28] M. Jelali and A. Kroll, "Hydraulic servo systems: Modelling, identification and control," pp. 53–126, Springer-Verlag London, 2003.

Part II

Budget

Table of Contents

For the realization of this project different cost and expenses were needed. This report tries to explain and summarize all of them in order to have an idea of the total budget.

1 Labour Cost

Inside this cost, a differentiation is made between to different types of labour cost; direct and indirect labour cost. The former is the wages paid to the engineered hired working full time in the project. The latter is considered all the indirect people that contribute to the project who need to be paid for the job provided.

1.1 Direct Labour Cost

An engineer working full time is required, eight hours per day from Monday to Friday over a period of six months. The average salary is set in 1500€ per month. Thus, after at the end of the period the direct labour cost is 9000€ Indirect Labour Cost The services of different experts were used for the realization of the project:

- Software Engineer: one day per week during two month a two hours meeting was held with an engineer from the valve provider company. This meeting had the purpose of solving different issues with the valve internal software due to the lack of information and experience with it at the beginning. His services have an estimated cost of 35€ per hour being the total cost over 576€.
- Lab Technician: a lab technician was available for setting up and doing different maintenance operation of the system. Considering that the average salary for the technician is 1300€ and over the six month just a five percent of his time was expend in the project, the cost due to the technician services is around 400€.
- dSPACE Tutorial: an expert in dSPACE hardware provided a tutorial for three hours. It was mainly and introduction for using the hardware. The cost of this service was 150€.

1.2 Summary Labour Cost

The table following summarized all the cost explained above.

Direct Labor Cost			
Throwput	Description	Unit Cost (€)	Total Cost (€)
6	mo. Fultime Engineer	1500	9000
Direct Labor Cost			
Throwput	Description	Unit Cost (€)	Total Cost (€)
16	hr. Software Engineer	36	576
49,24	hr. Lab Tecnician	8,13	400,32
3	hr. Tutorial dSPACE	50	150
Total Labor Cost			10126,32

2 Manufacturing Material Cost

Although the main focus of the project was developing a digital controller for the suspension system, different materials were needed:

- Position Sensor Cable: four Sensor cable M12 were needed in order to be able to connect the sensor to the dSPACE box. The price for each cable is 16€.
- Ribbon Cable: this cable was used for creating a CAN network. A 30 meter long roll was bought for a price of 60€.
- Housing Case: A low pass filter was designed for filtering the noise coming from the sensors. The PCB was housed in a case with a price of 15€

Manufacturing Material Cost			
Units	Description	Unit Cost (€)	Total Cost (€)
4	Position Sensor Cable	16	64
1	30m Roll Ribbon Cable	60	60
2	Housing Case	15	30
Total Manufacturing Material Cost			154,00

3 Software Cost

Several licenses were used during the project:

- Microsoft Office: the price for a whole year license is 100€. Since the project lasted for 6 months the price regarding the license is 50€.
- Matlab and Simulink: including all the toolboxes needed, the total amount is 7000€. Considering that the license is renewed every four years and that it was fully used by this project for six months, the cost is 875€.

- dSPACE: the license for the hardware and software with the configuration used was 70000€. Considering that the license and hardware is renewed every ten years and that is was fully used for six months, the cost for this project is 3500€.

Sofware Cost			
Fraction used	Description	Unit Cost (€)	Total Cost (€)
0,5	Microsoft Office	100	50
0,13	30m Roll Ribbon Cable	7000	875
0,05	Housing Case	70000	3500
Sofware Cost			4425,00

4 Office Material Cost

- Paper: different copies of articles and datasheet were printed during the project. Two packets of 500 A4 sheets were used. The unit price for each packet is around 3.5€
- Office Computer: A computer was needed for office work such as writing, reading articles, creating presentation, etc. Since this task are not demanding, the cost of the computer used was around 400€. The life time for this type of computer is over 6 years. Since this project last for 6 months, the cost inferred by it is around 34€.
- Testing Computer: A computer with more computational power was used for moving the testing tools and handle large amount of date. The cost of this computer was around 1200€. Due to the fast developing of both hardware and software, the life time of this computer is estimated to be 4 years. The proportional cost added to the project from this item is 150€

Office Material Cost			
Throwput	Description	Unit Cost (€)	Total Cost (€)
2	units A4 paper packets	3,5	7
0,09	Office Computer	400	34,4
0,125	Testing Computer	1200	150
Office Material Cost			191,40

5 Communication and Shipments

As it was mentioned above, a phone call of two hours was made each week for the first two months of the project. This call was made from Sweden to Denmark. Considering that the price for an international call was 0.1€, the price for a single call was 12€

Due to technical problems with the valves, two of them (in separated shipments) were sent to the manufacturing company. The price per shipment was 60€.

Comunication and Shipments			
Units	Description	Unit Cost (€)	Total Cost (€)
8	International Call	12	96
2	Valve Shipment	60	120
Office Material Cost			216

6 Other Expenses

- Trip to the test track: a trip was made in order to see the track is used for testing the different devices of a forwarder in which is include the cab suspension. The purpose of this trip was giving a better idea of the suspension concept. The trip included journey which was 40€ plus lunch, 15€. Total sum 55€.
- Lunches with the Stakeholders: two lunch for four people were held with the coordinators and stakeholders of the project. The final intend of this lunches were to keep update all people involved in the project plus receiving feedback of the work done. The cost per lunch was 50 €

Other Cost			
Units	Description	Unit Cost (€)	Total Cost (€)
1	Test Track Trip	55	55
2	Lunches	50	100
Other Cost			155

7 Overall Cost and Tender Budget

In the following table is shown a summary of the cost previously introduced. In order to obtain the tender budget needed for the project it has been consider a general cost of 12%, 6% of profit of the project and a 25% of taxes (VAT). The final Tender Base Budget is 22657.30€

Overall Cost	
Issue	Cost (€)
Labour cost	10126,32
Manufacturing Material Cost	154,00
Sofware Cost	4425,00
Office Material Cost	191,40
Comunication and Shipments Cost	216,00
Other Cost	155,00
General Cost	1832,126544
Sum of Costs	17099,85
6% of Benefit	1025,99
Contracted Operation Budget	18125,84
25% of Taxes	4531,46
Tender base budget	22657,30

Part III

Appendix

List of Figures

Forwarder Dimensions

TECHNICAL SPECIFICATIONS

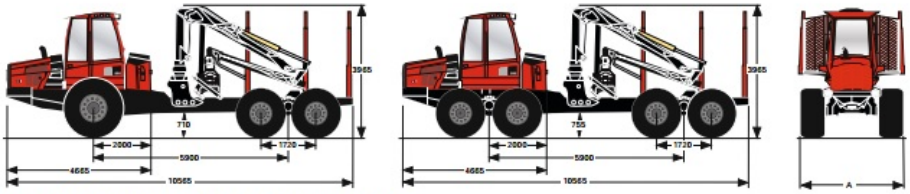

Machine dimensions with the shortest of the four rear frame alternatives.

WHEEL EQUIPMENT ALTERNATIVES, FRONT AND REAR, AND MACHINE WIDTH (A)

	Tire	Width (mm)
6 WD (front)	710/70x34	3,060
6 WD (rear)	780/50x28.5	3,160
8 WD (front/rear)	780/50x28.5	3,160

NOTE: Stated dimensions are nominal and may vary slightly depending on production tolerances.

WEIGHT

	6 WD	8 WD
Weight from:	20,700 kg	23,800 kg

ENGINE

	74 AWI-4V, 6-cyl. diesel engine with turbo and intercooler. EPA Tier 4i and EU stage 3B. DEF/SCR post-treatment. (Stage II/EPA Tier 2 for Russia, Australia and South America)
Stroke volume:	7.4 l
Power, max.:	193 kW DIN (259 hp) at 1700 RPM.
Torque:	1100 Nm at 1200-1700 RPM.
Fuel tank:	210 l
DEF tank:	18 litres
Miscellaneous:	Water separator. Fuel filter. Throttle, electrical via CAN. Thermostat-controlled fan (electric). Electrical refuelling.

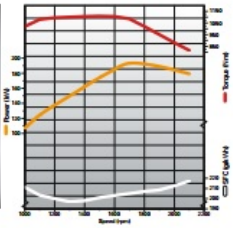

TRANSMISSION

	Computer-controlled, hydrostatic mechanical transmission. 6/8-wheel drive. Transfer case with 2 positions (high and low). Disengageable drive operation.
Driving speed:	0-20/21 km/h (without/with steering wheel)
Pulling force:	26,000 kp (255 kN)

FRAME/AXLES

	Four rear frame alternatives. Frame with smooth V-shaped bottom made of high-strength steel.
Ex. of other equipment:	Front blade. Stabiliser. Towing point, rear.

HYDRAULIC SYSTEM

	Single circuit load-sensing system with variable piston pump.
Flow:	360 l/min at 2000 RPM
Max. working pressure:	24.5 MPa (245 bar)
Hydraulic oil reservoir:	167 l
Miscellaneous:	Pressure filter for hydrostatic circuit. Dual return oil filters for hydrostatic and working hydraulics. Hydraulic oil level warning. Sight glass level control. Contamination indication for return oil filter. Visual alarm in cab.

BRAKE SYSTEM

	Fully hydraulic multi-disc brakes. Hydraulic accumulator charging valve.
Driving brakes/ Working brake:	Multi-disc brakes in oil bath. Automatically engaged when working.
Parking brake:	Spring-action brake with electro-hydraulic control. Emergency brake.
Braking performance:	Conforms to ISO 11169 and VVFS 2003:17.

CAB/ERGONOMICS

	Safety tested. Spacious and bright with very good visibility. Thermal and acoustic insulation.
Safety:	Conforms to ISO 8082-1 (ROPS), ISO 8083 (FOPS) and ISO 8084 (OPS). Alternative cab that also conforms to WCB OPS G603.
Seat:	Three alternative seat selections. Ergonomically designed with head rest, arm rests, joystick panels and waist safety belt. Depending on seat selection, different capabilities are available for individual adjustment of the seat cushion, back rest and lumbar support. Seat column with 0–180-degree working range.
Windshields:	Protective glass in side windows and rear window. Alternative cab conforming to WCB OPS G603, with protective glass in all windows.

Simulink Models

Theoretical model for one Cylinder

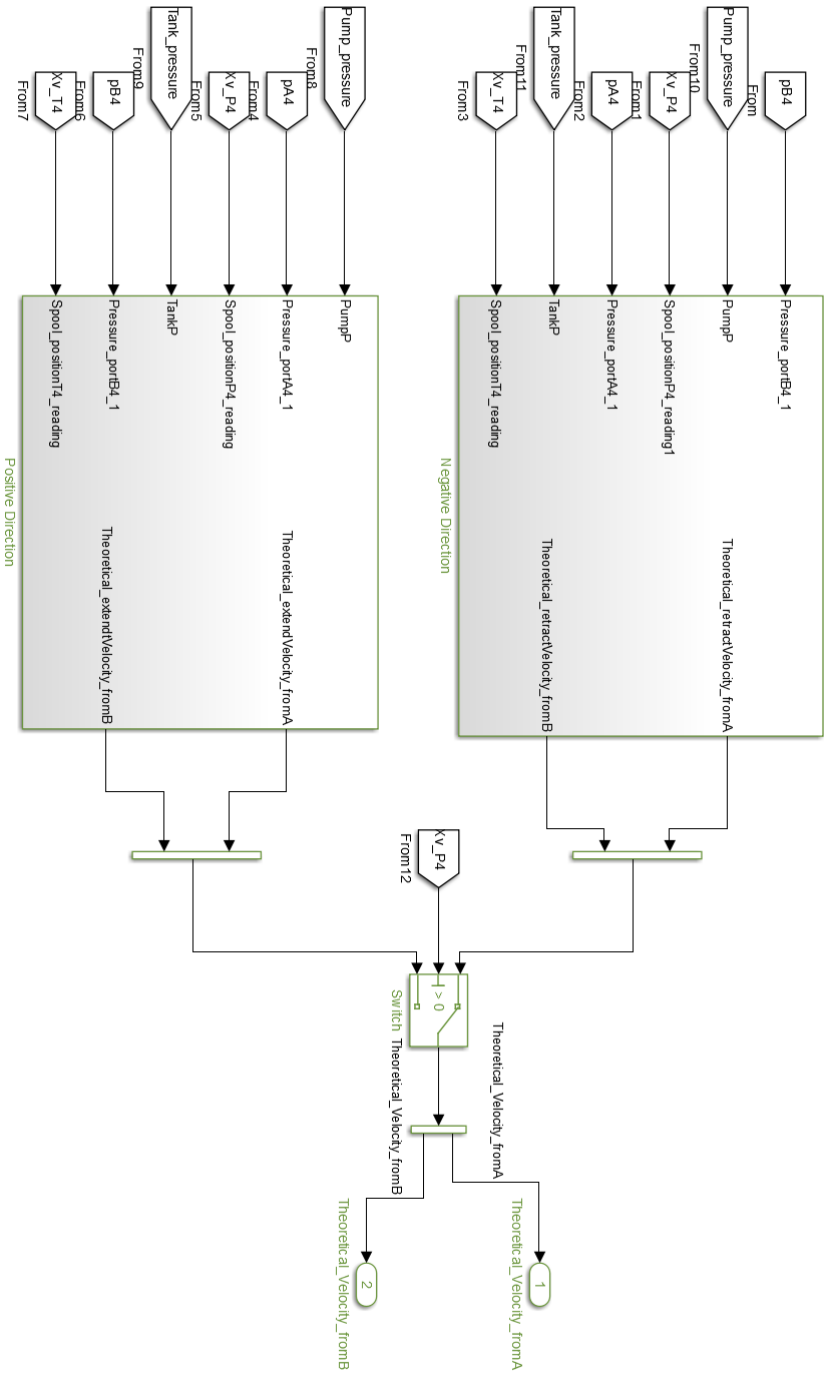

Figure 49: Theoretical Simulink Model

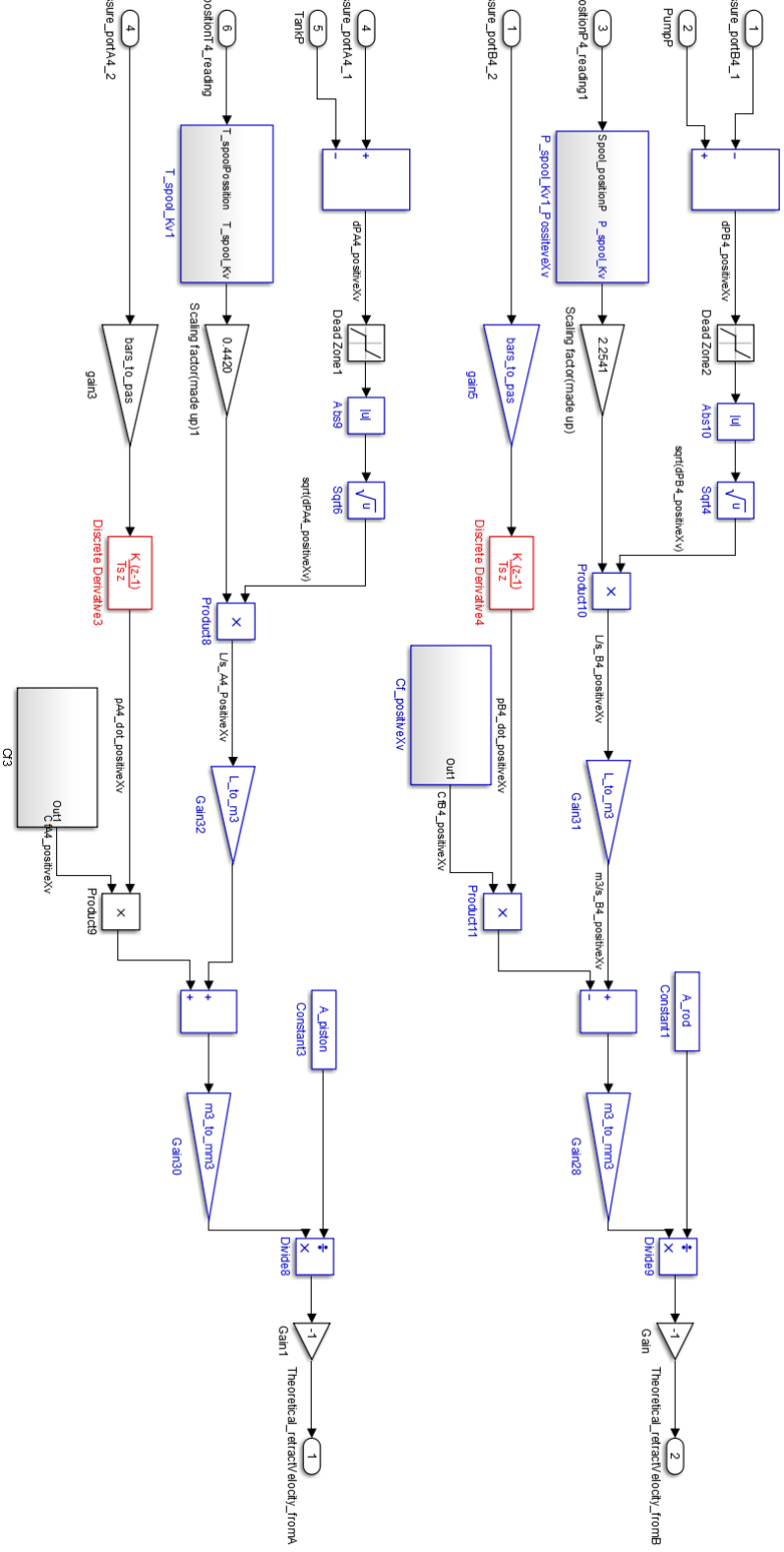

Figure 50: Detailed Simulink Model for retraction of the actuator

Actuator Controller

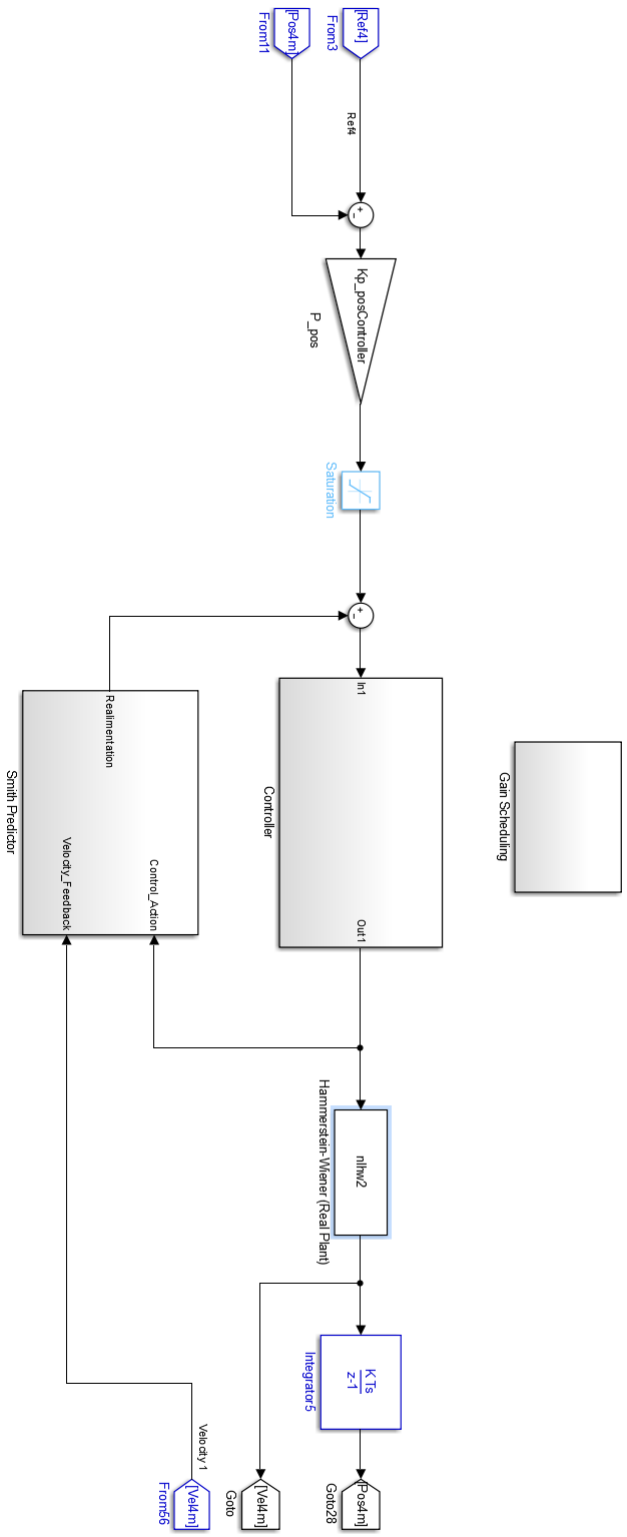

Figure 51: Actuator controller Simulink block model

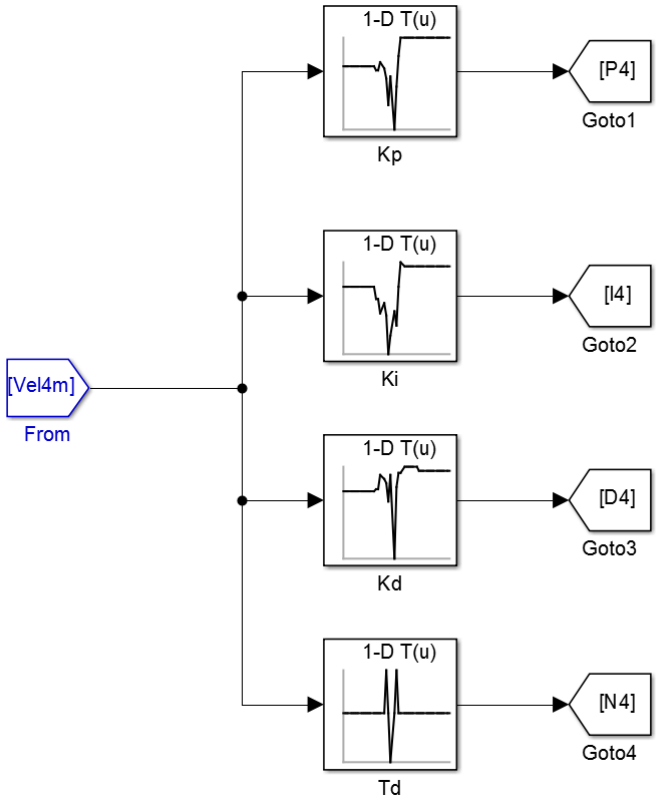

Figure 52: Gain Scheduling Simulink block model

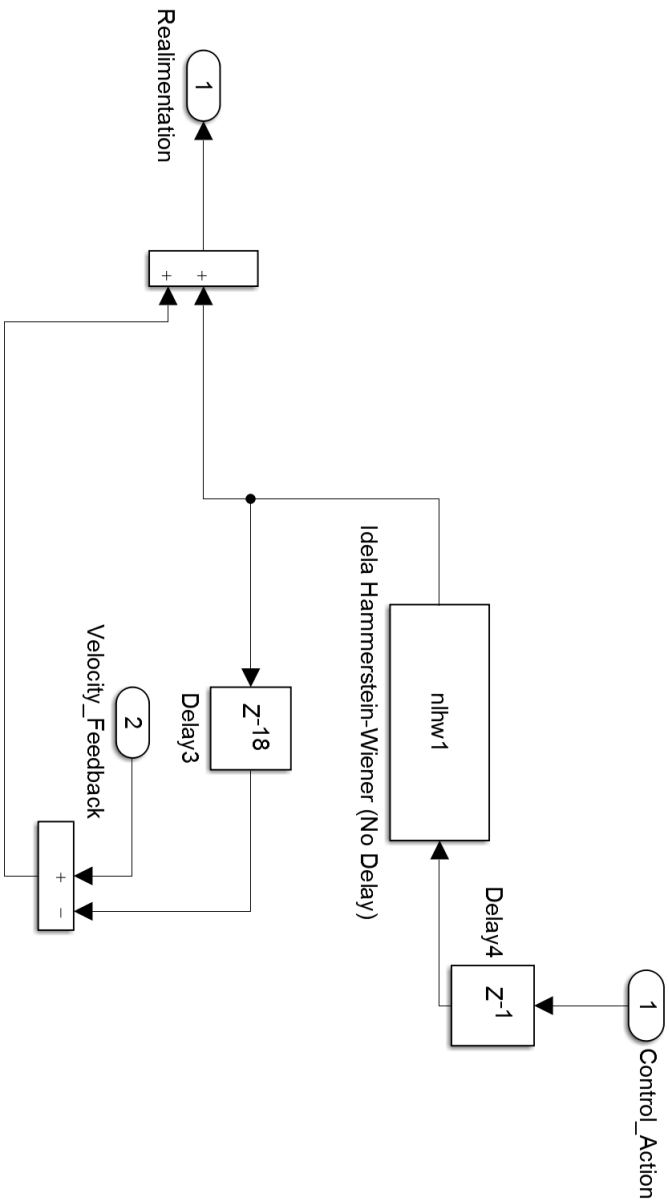

Figure 53: Smith Predictor Simulink block model

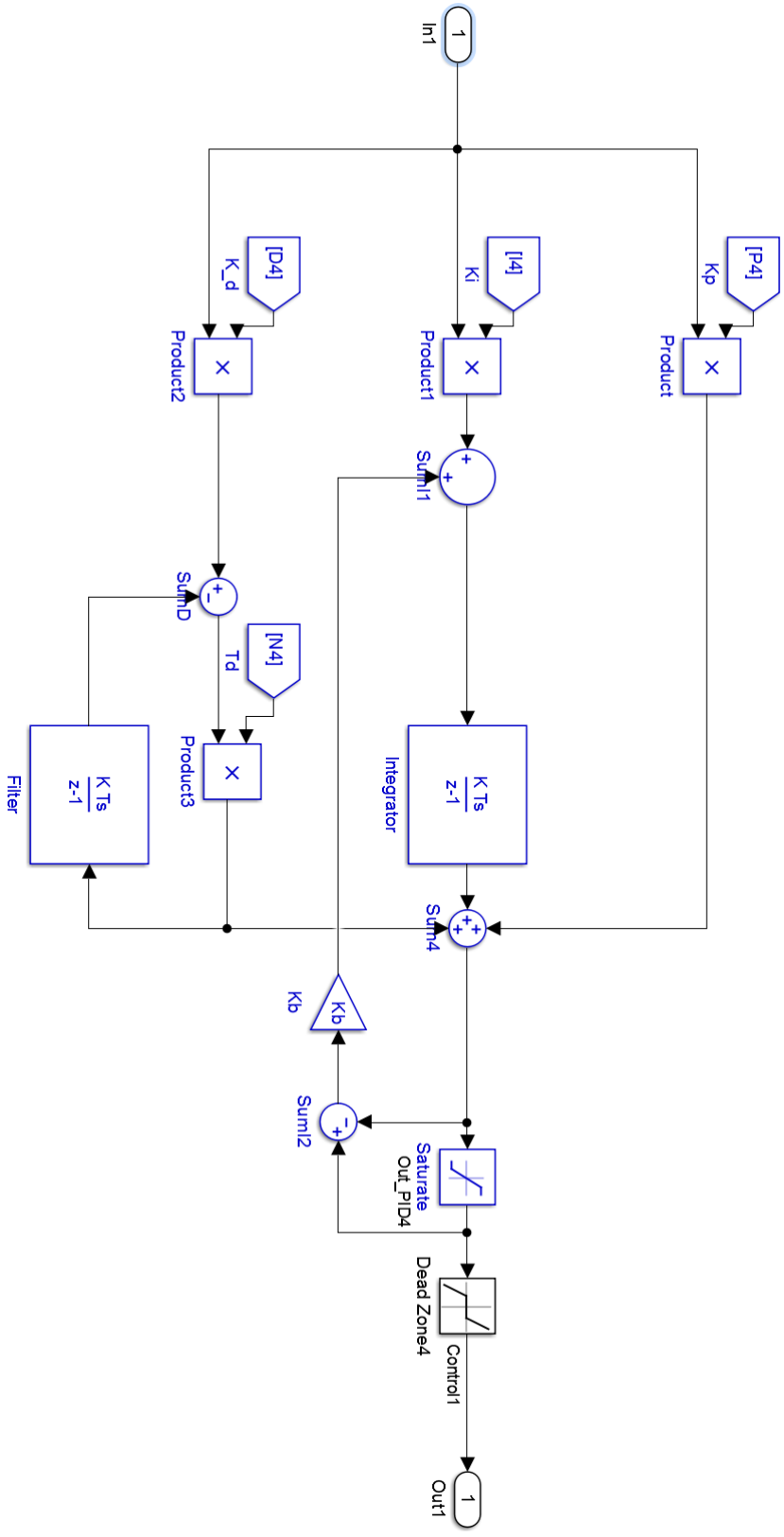

Figure 54: Controller Simulink block model

Pump Datasheet

Axial Piston Pump
Series PV

Variable Displacement

Catalogue HY30-3243/UK
April 2006

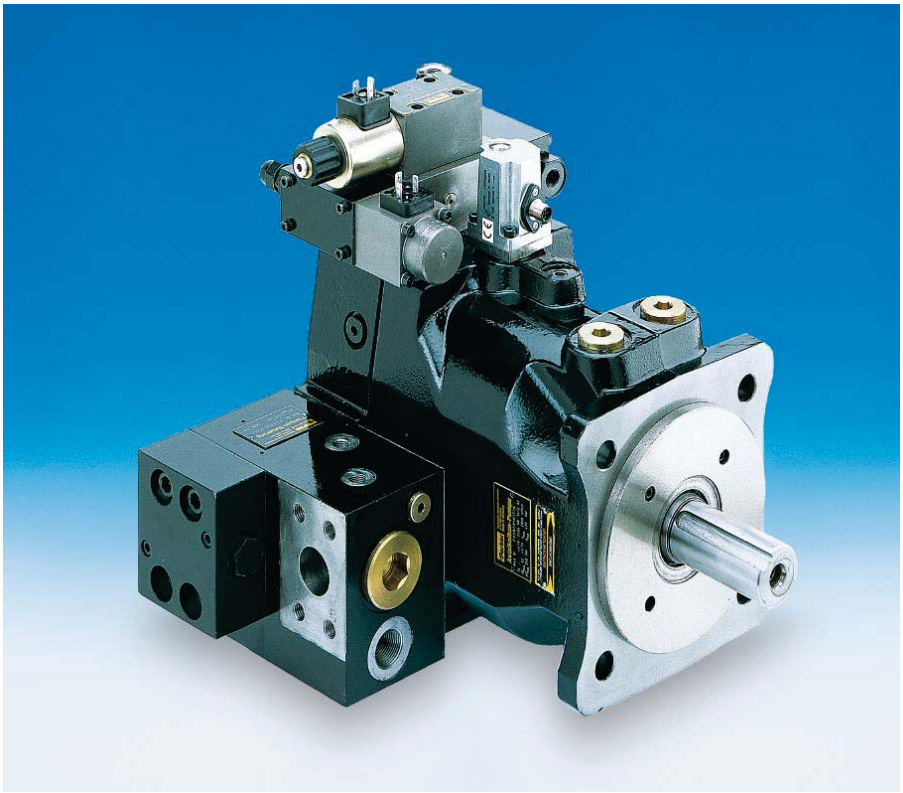

Pump with Standard Pressure Compensator, code F*S

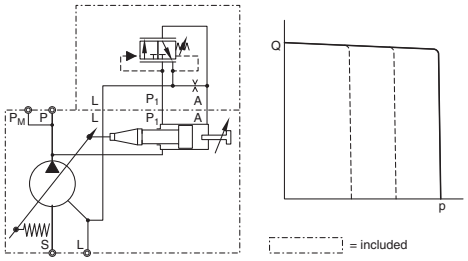

Pump with Load-Sensing Compensator, code FFC

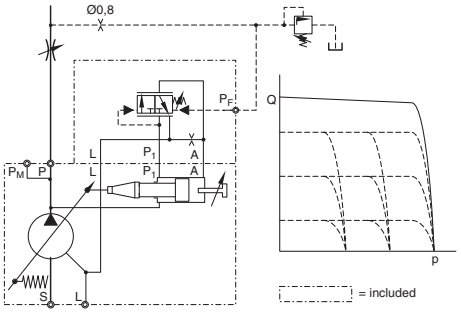

With thru drive for single and multiple pumps

Swash plate type for open circuit

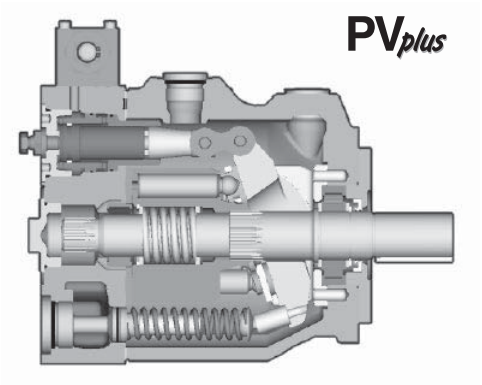

Technical Features

- Mounting interface according to VDMA-standards sheet 24560 part 1
- Standard: 4-hole flange ISO 3019/2 (metric)
- Large servo piston with strong bias spring achieves fast response; e.g. for PV042
  upstroke < 75 ms
  downstroke < 45 ms
  Note: Follow installation instructions.
- Reduced pressure peaks due to active decompression of system at downstroke
- Also at low system pressure reliable compensator operation. Lowest compensating pressure 12-15 bar
- 9 piston and precompression technology (precompression volume) result in unbeaten low outlet flow pulsation.
- Rigid and FEM-optimized body design for lowest noise level
- Complete compensator program
- Thru drive for 100% nominal torque

Pump with Power Compensator, code *LB

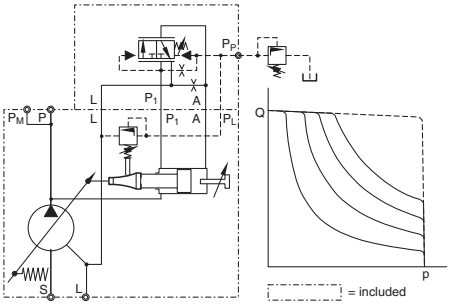

Pump with Electrohydr. Displacement Control, code FPV

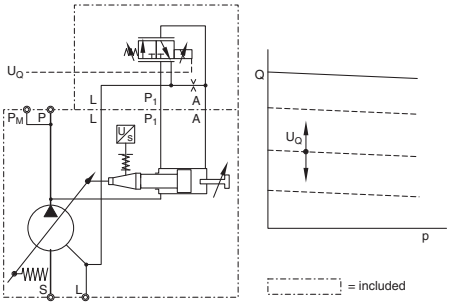

Technical data

Displacement	[cm^3/rev]	from 16 to 270
Operating pressures		
Outlet	[bar]	nominal pressure p_N 350
	[bar]	max. pressure $p_{max.}$ 420 1)
	[bar]	drain port 2 2)
Inlet min.	[bar]	0.8 (absolute)
max.	[bar]	16
Minimum speed	[min^{-1}]	300 min^{-1}
Mounting interface		4-hole flange ISO 3019/2
Installation		drain port as high as possible

1) max. 20% of working cycle
2) peak pressure only


Pump with Standard Pressure Comp.

Pump with Power Comp.


Combination PV/PV

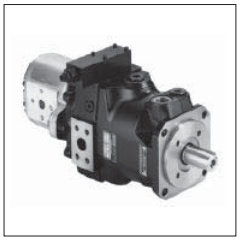
Combination PV/PGP

Selection table

Model	Max. displacement [cm^3/rev]	Output flow at 1500 min^{-1} [l/min]	Input power at 1500 min^{-1} and 350 bar [kW]	Max speed * [min^{-1}]	Moment of inertia [kgm^2]	Weight [kg]
PV016	16	24	15.5			
PV020	20	30	19.5	3000	0.0017	19
PV023	23	34.5	22.5			
PV063	63	94.5	61.5	2800		
PV080	80	120	78	2500	0.018	60
PV092	92	138	89.5	2300		
PV140	140	210	136	2400	0.030	90
PV180	180	270	175	2200		
PV270	270	405	263	1800	0.098	172

* The maximum speed ratings are shown for an inlet pressure of 1 bar (absolute) and for a fluid viscosity of ν = 30 mm^2/s.

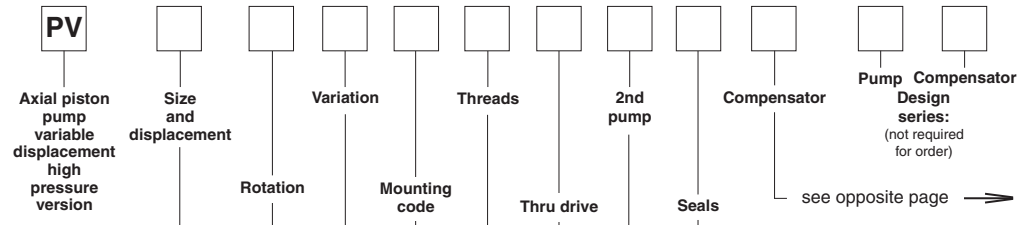

Code	Displacement
016	**16 cm³/rev**
020	**20 cm³/rev**
023	**23 cm³/rev**
063	**63 cm³/rev**
080	**80 cm³/rev**
092	**92 cm³/rev**
140	**140 cm³/rev**
180	**180 cm³/rev**
270	**270 cm³/rev**

Code	Rotation [1]
R	**Clockwise**
L	Counter clockwise

[1] When looked on shaft

Code	Variation
1	**Standard**
9	Reduced displacement adjusted [2]

[2] For order specify displacement.

Code	Mounting interface		Shaft
D	SAE ISO 3019/1	4-hole flange	Cylindric, key
E		4-hole flange	Splined, SAE
F[3]		4-hole flange	Cylindric, key
G[3]		4-hole flange	Splined, SAE
K	**metr. ISO 3019/2**	**4-hole flange**	**Cylindric, key**
L		**4-hole flange**	**Splined, DIN 5480**

[3] Codes F and G only for PV140/180, see dimension sheet

Code	Port [4]	Threads[5]
1	**BSPP**	**Metric**
3	UNF	UNC
4[6]	BSPP	Metr. M14
7	ISO 6149	UNC
8	ISO 6149	Metric[1]

[4] Drain, gauge and flushing ports
[5] All mounting and connecting threads
[6] For PV063-PV180 only: pressure port 1 1/4" with 4 x M14 instead of 4 x M12

Code	Seals
N	**NBR**
V	FPM
E	EPDM
W	NBR with PTFE shaft seal
P	FPM with PTFE shaft seal
S	EPDM with PTFE shaft seal

Code	2nd pump option[7]
1	**Single pump, no 2nd pump and coupling**
2	PV140 or PV180 mounted
3	PV or PVM pump mounted
4	Gear pump series PGP mounted

[7] Specify 2nd pump with full model code

Code	Thru drive option no adaptor for 2nd pump
T	**Single pump prepared for thru drive**
	With adaptor for 2nd pump
Y[8]	SAE AA, Ø 50.8mm
A	SAE A, Ø 82.55mm
B	SAE B, Ø 101.6mm
C[9]	SAE C, Ø 127mm
D[10]	SAE D, Ø 152.4mm
E[11]	SAE E, Ø 165.1mm
G[12]	Metric, Ø 63mm
H	Metric, Ø 80mm
J	Metric, Ø 100mm
K[9]	Metric, Ø 125mm
L[10]	Metric, Ø 160mm
M[11]	Metric, Ø 200mm

[8] Only for PV016 - PV023
[9] Only for PV032 and larger
[10] Only for PV063 and larger
[11] Only for PV270
[12] Only for PV016 - PV092

Bold letters =
Short-term availability

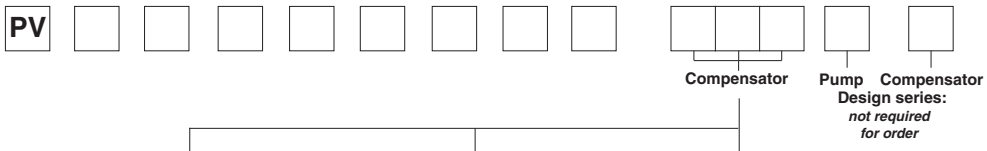

Standard Pressure Compensator			
Code_			Compensator options
0	**0**	**1**	**No compensator**
1	**0**	**0**	**With coverplate, no control function**
F	**D**	**S**	**10 - 140 bar, spindle + lock nut**
F	**H**	**S**	**40 - 210 bar, spindle + lock nut**
F	**W**	**S**	**70 - 350 bar, spindle + lock nut**
			Remote Compensator options
F	**R**		**Remote pressure compensator**
F	S		Variation R, for quick unload valve
F	**F**		**Load-Sensing compensator**
F	T		Two valve load-sensing compensator
			Variations for Remote Compensator
		C	**External pressure pilot [13)]**
		1	**NG6/D03 interface top side**
		2	**Like 1 but with ext. pilot port [15)]**
		P	**Pilot valve PVAC1P* mounted**
		D	Proportional pilot valve type PVACPP* mounted
		L	Pilot valve with DIN lock mounted
		Z	Accessory mounted [14)]

Power compensator								
Code			Displacement					Compensator option
			016 023	063 092	140	180	270	Nom. power [kW] at 1500 min^{-1} / Nom. torque [Nm]
B			x					3 / 19.5
C			x					4 / 26
D			x					5.5 / 36
E			x					7.5 / 49
G			x	x				11 / 71
H			x	x				15 / 97
K			x	x	x			18.5 / 120
M				x	x	x		22 / 142
S				x	x	x		30 / 195
T				x	x	x	x	37 / 240
U				x	x	x	x	45 / 290
W				x	x	x	x	55 / 355
Y					x	x	x	75 / 485
Z					x	x	x	90 / 585
2						x	x	110 / 715
3							x	132 / 850
			Function					
	L		x	x	x	x	x	Power compensator
	C		x	x	x	x	x	Power compensator and load-sensing
			Variation					
		A	x	x	x	x	x	NG6 interface top side
		B	x	x	x	x	x	No pressure compensation
		C	x	x	x	x	x	Adjustable pressure compensation
		D	x	x	x	x	x	Proportional pilot valve PVACPP* mounted
		Z	x	x	x	x	x	Accessories mounted [14)]

Electrohydraulic compensator			
Code			Compensator option
			Pilot pressure supply
F			Standard (internal), no shuttle valve
U			Elbow manifold, compensator horizontal [16)]
			Function
	P		Proportional displacement control
			Variation
		V	Standard, no pressure compensation
		R	Remote pressure comp. NG6 interface
		G	Variation R, Pressure sensor and proportional pilot valve mounted for pressure resp. power control
		D	Variation R, Proportional pilot valve PVACPP* mounted
		Z	Variation R, accessories mounted [14)]
		S	Remote pressure comp., NG6 interface top side, for quick unload valve
		T	Variation S, pressure sensor and proportional pilot valve mounted for pressure resp. power control
		P	Remote pressure comp., NG6 interface top side, for preload and quick unload manifold
		E	Variation P, pressure sensor and proportional pilot valve mounted for pressure resp. power control

[16)] not for *UPV

Note

Compensator differential Δp is to be adjusted:

Remote pressure comp., power comp. 15 ± 1 bar
(Codes FR*, FT*, *L*, *C*, FPR, FPD, FPZ, FPG)

With quick unload manifold 12 ± 1 bar
(Codes FS*, FPS, FPT, FPP, FPE)

Load-Sensing comp. (not power comp.) 10 ± 1 bar
(Codes FF*)

The ordering code PVACPP* correspond to the DSAE1007P07*

[13)] Not for two-valve-compensator

[14)] Accessories not included, please specify on order with full model code.

[15)] Only for Codes *FR* and *FT*

Bold letters =
Short-term availability

PV016 - PV023

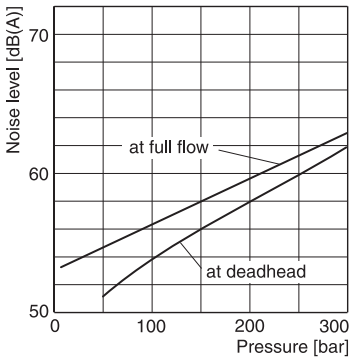

PV180

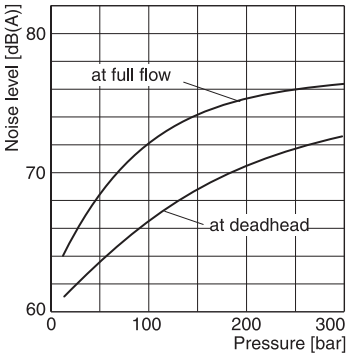

PV063 - PV092

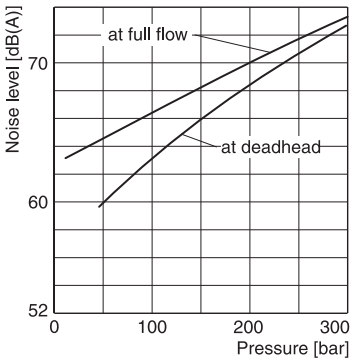

PV270

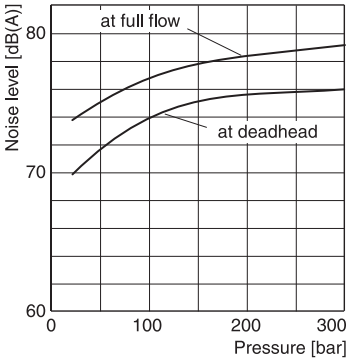

PV140

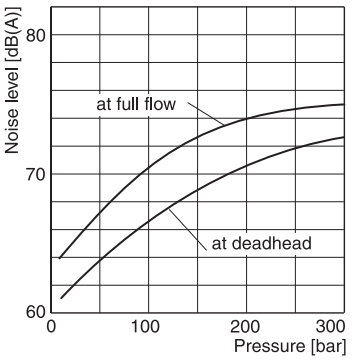

Typical sound level for single pumps, measured in unechoic chamber according to DIN 45 635, part 1 and 26. Microphone distance 1m; speed: n = 1500 min-1.

All data measured with mineral oil viscosity 30 mm²/s (cSt) at 50°C.

Efficiency, power consumption
PV063

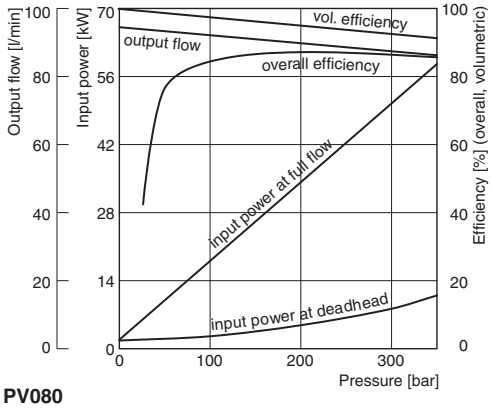

PV080

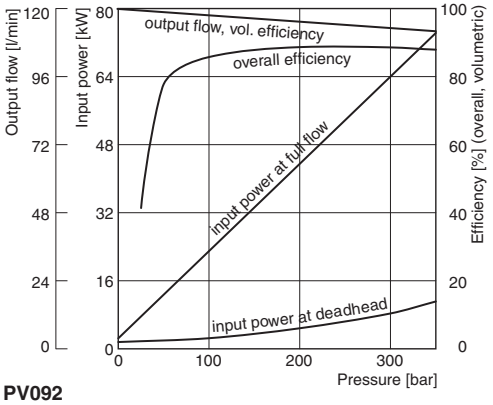

PV092

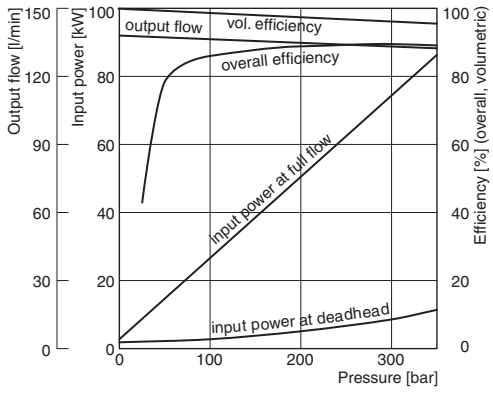

Efficiency and case drain flows PV063, PV080, PV092

The efficiency and power graphs are measured at an input speed of n = 1500 min^{-1}, a temperature of 50 °C and a fluid viscosity of 30 mm^2/s.

Case drain flow and compensator control flow leave via the drain port of the pump. To the values shown are to be added 1 to 1.2 l/min , if at pilot operated compensators (codes FR*, FF*, FT*, power compensator and p-Q-control) the control flow of the pressure pilot valve also goes through the pump.

Please note: The values shown below are only valid for static operation. Under dynamic conditions and at rapid compensation of the pump the volume displaced by the servo piston also leaves the case drain port. This dynamic control flow can reach up to 80 l/min! Therefore the case drain line is to lead to the reservoir at full size and without restrictions as short and direct as possible.

Case drain flows PV063-092

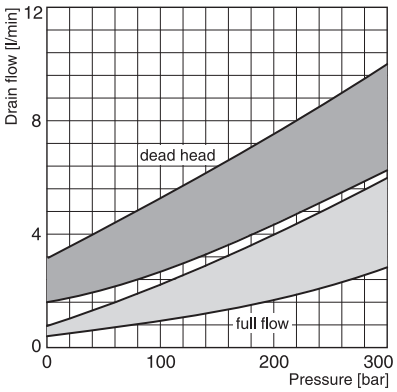

PV063 - 092, metric version

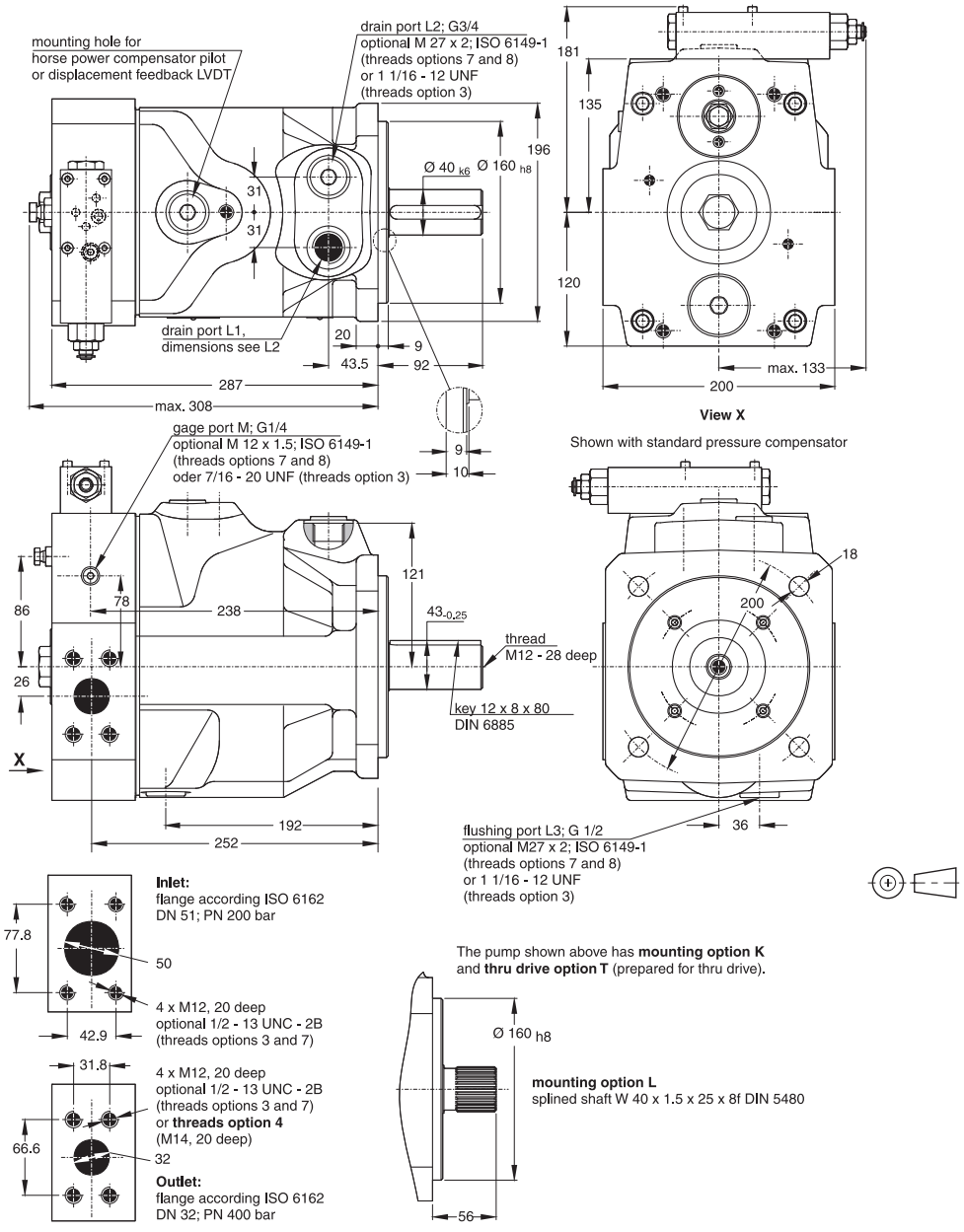

For further information about flanges see catalogue No. 4039/UK „Pressure Hydraulic Flanges“ (on request).
Shown is a clockwise rotating pump. Counter clockwise rotating pumps have inlet, outlet and gauge ports reversed.

PV063 - 092, SAE version and thru drive version

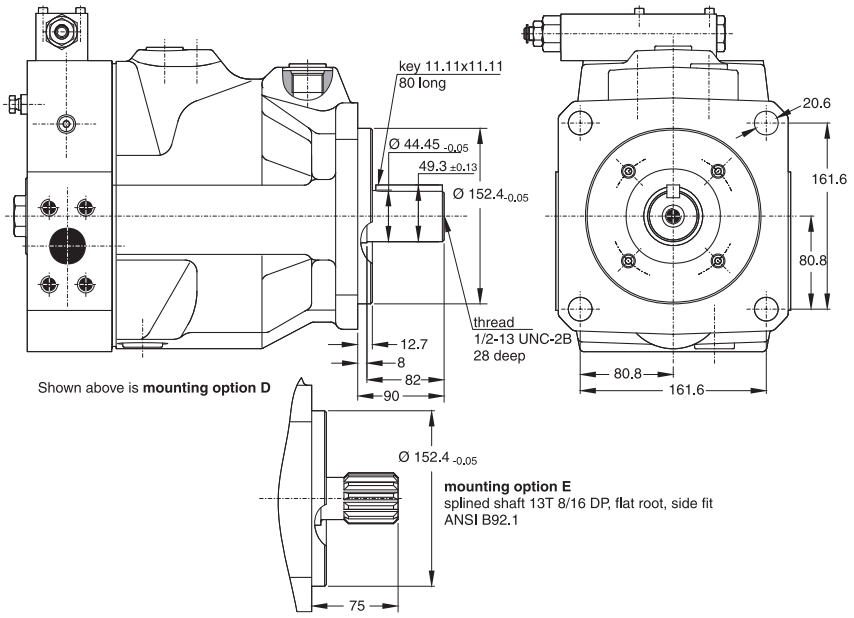

Variation with thru drive

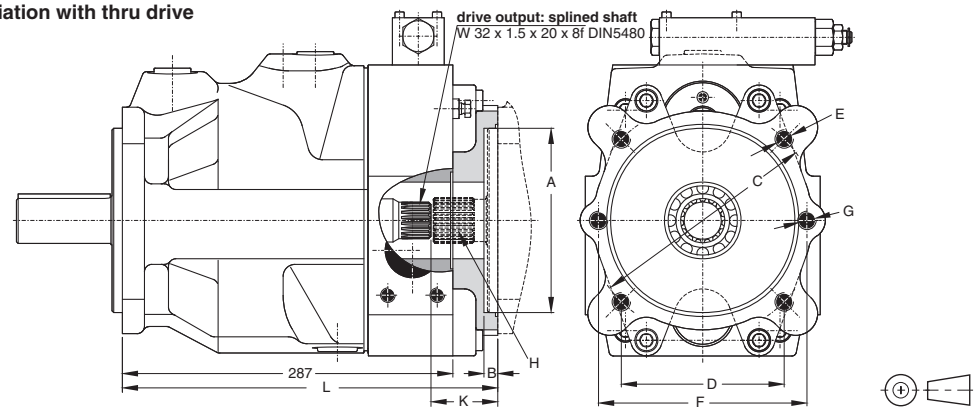

Thru shaft adaptors are available with the following dimensions:								
A	**B**	**C**	**D**	**E**	**F**	**G**	**K**	**L**
63	10	85	-	M8	100	M8	58	326
80	10	103	-	M8	109	M10	58	326
100	12	125	-	M10	140	M12	58	326
125	12	160	-	M12	180	M16	58	326
160	12	200	-	M16	-	-	58	326
82.55	10	-	-	-	106	M10	58	326
101.6	12	-	89.8	M12	146	M12	58	326
127	14	-	114.5	M12	181	M16	58	326
152.4	14	-	161.6	M16	-	-	78	346

Dimension H and available couplings see page 24.
At threads options 3 and 7 the dimensions E and G are UNC - 2B threads.